Title:

Docosahexaenoic acid reduces microglia phagocytic activity via miR-124 and induces neuroprotection in rodent models of spinal cord contusion injury

Authors:

Ping K. Yip[1*], Amy L. Bowes[1], Jodie C.E. Hall[2], Miguel A. Burguillos[1], TH Richard Ip[1], Tracey Baskerville[1], Zhuo-Hao Liu[1,3], Moumin A.E.K. Mohamed[1], Fanuelle Getachew[1], Anna D. Lindsay[1], Saif-Ur-Rehman Najeeb[1], Phillip G. Popovich[2], John V. Priestley[1] & Adina T. Michael-Titus[1]

Affiliations:

[1] Centre for Neuroscience, Surgery and Trauma, Blizard Institute, Barts and The London School of Medicine and Dentistry, Queen Mary University of London, London E1 2AT, U.K.

[2] Centre for Brain and Spinal Cord Repair, Department of Neuroscience, Wexner Medical Center at The Ohio State University, Columbus, OH, USA

[3] Chang Gung Medical College and University, Chang Gung Memorial Hospital, Department of Neurosurgery, 5 Fu-Shin Street, Linkou, Taiwan

Corresponding author:

Dr Ping K. Yip

Centre for Neuroscience, Surgery and Trauma,

Blizard Institute,

Barts and The London School of Medicine and Dentistry,

Queen Mary University of London,

London E1 2AT, U.K.

Tel: (0)20 7882 2273

Fax: (0)20 7882 2180

Email: p.yip@qmul.ac.uk

Abstract

Microglia are activated after spinal cord injury (SCI), but their phagocytic mechanisms and link to neuroprotection remain incompletely characterised. Docosahexaenoic acid (DHA) has been shown to have significant neuroprotective effects after hemisection and compression SCI, and can directly affect microglia in these injury models. In rodent contusion SCI, we demonstrate that DHA (500 nmol/kg) administered acutely post-injury confers neuroprotection and enhances locomotor recovery, and also exerts a complex modulation of the microglial response to injury. In rodents, at 7 days after SCI, the level of phagocytosed myelin within Iba1-positive or P2Y12-positive cells was significantly lower after DHA treatment, and this occurred in parallel with an increase in intracellular miR-124 expression. Furthermore, intraspinal administration of a miR-124 inhibitor significantly reduced the DHA–induced decrease in myelin phagocytosis in mice at 7 days post SCI. In rat spinal primary microglia cultures, DHA reduced the phagocytic response to myelin, which was associated with an increase in miR-124, but not miR-155. A similar response was observed in a microglia cell line (BV2) treated with DHA, and the effect was blocked by a miR-

124 inhibitor. Furthermore, the phagocytic response of BV2 cells to stressed neurones was also reduced in the presence of DHA. In peripheral monocyte-derived macrophages, the expression of the M1, but not the M0 or M2 phenotype, was reduced by DHA, but the phagocytic activation was not altered. These findings show that DHA induces neuroprotection in contusion injury. Furthermore, the improved outcome is via a miR-124-dependent reduction in the phagocytic response of microglia.

Introduction

Spinal cord injury (SCI) is a significant cause of disability worldwide, affecting approximately 130,000 people annually (1). Despite extensive research, there is still no effective treatment and the various cascades of secondary pathology post-injury are poorly understood. SCI is associated with a strong inflammatory response, and microglia, resident central nervous system (CNS) immune cells, become activated immediately after injury (2, 3). Activated microglia take on an

amoeboid-like morphology that facilitates their migration to the site of the injury, where they release a range of cytotoxic mediators (4, 5). Although activated microglia have many similarities with monocyte-derived macrophages, they also have differences at the genetic and phenotypic levels (6). Furthermore, microglia have been shown to induce a form of primary phagocytosis, termed phagoptosis, of stressed but viable neuronal cells (7-9). However, microglia are also known to act as sources of anti-inflammatory mediators and neurotrophic factors, aiding CNS repair (10, 11). Microglia initiate both innate and adaptive immune cell responses post-SCI via pro-inflammatory cytokine release and major histocompatibility complex (MHC) II antigen expression (5, 12). Therefore, microglia exhibit a wide range of functions, which can be neurotoxic or neuroprotective.

A robust and protracted macrophage response accompanies microglial activation after SCI. Whilst acute depletion or inhibition of CNS macrophages is neuroprotective (13, 14), augmentation of this immune cell response can also, paradoxically, lead to CNS repair (15, 16). These divergent effects of activated microglia/macrophages might be explained by the induction of functionally separate phenotypes, such as the classically activated (M1) and alternatively activated (M2) macrophage responses (3, 6). M1 macrophages produce high levels of pro-inflammatory cytokines and oxidative metabolites that are essential for host defence, but can also cause significant bystander damage (17, 18). On the other hand, the presence of interleukin (IL) IL-4 or IL-13 promotes the differentiation of M2 macrophages, which are responsible for several neuroprotective and reparative functions (19, 20). It is now well-documented that in the early phases of SCI, activated macrophages may acquire a short-lived M2 polarised phenotype, identified by the cell marker arginase-1 (arg-1), whereas chronic spinal cord inflammation is characterised by a strong

and persistent M1 polarised phenotype, identified by the presence of inducible nitric oxide-2 (iNOS-2) (21). Therefore, macrophage activity may exacerbate secondary injury or promote tissue repair post-SCI, depending on which subpopulation predominates, at different times after the initial injury.

The neuroprotective and macrophage/microglia modulatory effects of docosahexaenoic acid (DHA), and other closely related omega-3 polyunsaturated fatty acids such as eicosapentaenoic acid (EPA), have been well documented in compression and hemisection SCI (22-27). Although the exact pharmacological targets of omega-3 PUFAs driving their neuroprotective effects in SCI remain elusive, a range of beneficial effects have been reported after their acute administration post-injury in models of compression and hemisection injury, including decreased axonal and myelin damage, increased neuronal and oligodendrocyte survival, reduced lipid peroxidation and COX-2 activation, and improved locomotor recovery (22, 24, 25, 27-29). However, contusion injury represents a pathophysiologically different type of neurotrauma, and may better reflect human SCI than hemisection or compression injuries (30). We have recently shown, using in vivo positron emission tomography imaging in a rat contusion SCI model, that DHA can alter the levels of the translocator protein (TSPO), an inflammatory marker which is up-regulated in glia after injury (31).

In this study, we show that acute DHA treatment after injury promotes sustained locomotor recovery following spinal cord contusion injury in both rats and mice. This was accompanied by increased microglia/macrophage levels, but a reduced myelin phagocytosis, in parallel with an increase in microglial microRNA (miR)-124 expression. In vitro, DHA treatment reduces myelin phagocytosis in primary adult rat spinal microglia cultures and in the murine microglial cell line

BV-2. This phagocytic response appears to involve miR-124. The reduction in phagocytosis induced by DHA occurs in parallel with the neuroprotective effects, thus providing a mechanism that may be responsible for the beneficial effects of this fatty acid in contusion SCI.

Results

DHA improves open field locomotor scores in rodent spinal cord contusion injury

To assess the degree of motor functional loss and subsequent recovery in DHA-treated animals, the BBB and BMS open field locomotor rating scores were used to quantify recovery of hind limb function following contusion SCI in rats and mice, respectively. Using the scoring parameters mentioned in the methods section, both rats and mice showed complete paralysis of both hind limbs immediately following contusion SCI (Figure 1A-B). The injury paradigm used for rat SCI induced paralysis for only 1 day post-injury (BBB score of 0.6 for vehicle vs. 1.2 for DHA at 1 day post injury), indicating a moderate spinal contusion (Figure 1A). In the DHA-treated mice, a total paralysis (BMS score of 0) was observed for 3 days, whereas vehicle-treated mice were paralysed for 5 days post-injury, indicating a severe spinal contusion (Figure 1B). Although previous dose studies from our laboratory have shown that 250 nmol/kg DHA exerts significant neuroprotective effects in lateral hemisection and compression SCI in rats (22, 25, 32), 500 nmol/kg compared to 250 nmol/kg DHA exerted a more effective neuroprotection in compression-injured mice (24). Furthermore, preliminary studies in contusion injury in rats did not show significant differences in neuroprotection between 250 and 500 nmol/kg (data not shown). Therefore, to maintain similarity in the DHA dose between the rat and mouse contusion injury model, the higher DHA dose was chosen in this study, for both species. Intravenous administration

of DHA (500 nmol/kg) 30 minutes post-contusion SCI did not induce significantly different BBB scores in DHA- vs. vehicle-treated rats on days 0-4 post-contusion. However, significant improvement in locomotor recovery was observed from days 5 and 11 onwards, in rat and mouse models, respectively (Figure 1A-B). The enhanced locomotor recovery in DHA-treated rats and mice remained significant for up to 28 and 35 days post-contusion, respectively (Figure 1A-B). These data indicate that a single bolus injection of DHA (500 nmol/kg) can improve locomotor function during the early phase of recovery (7 days), with benefits sustained into the later phases of recovery (28 and 35 days), after moderate and severe contusion SCI in rodents.

DHA induces neuroprotection in rodent spinal cord contusion injury

The administration of DHA led to significantly improved neuronal survival on days 7 and 28 post-contusion injury in rats, as demonstrated by the number of neurons immunostained for the neuronal marker NeuN, around the injury epicentre (Figure 2A-J). In particular, significant neuroprotection in DHA-treated compared to the vehicle-treated rats was observed in the regions rostral and caudal to the epicentre at day 7 post-injury (Figure 2E-G), and regions caudal to the epicentre at day 28 post-injury (Figure 2H-J). Furthermore, significant neuronal survival was observed in DHA-treated mice, in the region rostral and caudal to the injury epicentre of the intermediate plane at 35 days post contusion, when compared to the vehicle-treated group (Figure 2K-S). These results show that DHA can protect against neuronal loss after a moderate or severe contusion of the cord.

DHA modulates microglia/macrophage activity in rodent spinal cord contusion injury

After SCI, there is an increase in activated microglia and the macrophage activation at the injury site (21, 22). In the present study, at 7 days post-contusion, DHA-treated rats displayed a small but significant increase in ED1 (a marker of activated microglia and monocyte-derived macrophages)

expression at 4 mm caudal to the epicentre when compared to control animals (Figure 3A-C). Immunostaining for Iba1, a marker that labels activated and non-activated microglia and macrophages, was also carried out. At 7 days post-contusion there was also a significant increase in Iba1-positive cells at the epicentre, and in regions rostral and caudal to the epicentre, in the DHA-treated group compared to vehicle-treated rats (Figure 3D-F). Interestingly, there was also an overall increase in the number of Iba1-positive cells in the white matter of mice at 35 days post severe spinal contusion injury after DHA-treatment, compared to the vehicle-treated group (Figure 3H-K, L). However, in the gray matter, the number of Iba1-positive cells was significantly reduced in the DHA-treated versus the vehicle-treated group (Figure 3M). However, at 28 days post moderate spinal contusion in rat, there was no significant difference in Iba-1 immunostaining between the two groups (Figure 3G). Furthermore, there was no significant difference when the gray and white matter data was combined, in the mouse contusion study (Figure 3N). These results demonstrate that DHA can modulate microglia/macrophages in both the white and gray matter caudal and rostral to the injury site after moderate-severe contusion.

DHA enhances both M1 and M2 microglia/macrophage phenotypes in spinal cord contusion injury

In order to further characterize the role of DHA in the modulation of activated microglia/macrophages after contusion of the cord, an additional analysis of microglia/macrophages using the CD16/32 and arginase-1 antibodies was carried out in mice and rats, at early or later stages of the SCI, to identify the two major subtypes of activated microglia/macrophage phenotype, namely M1 and M2.

As immunostaining with CD16/32 and arginase-1 antibodies on rat contused spinal cord sections was unsuccessful, these antibodies were instead used for Western blotting on freshly dissected tissue obtained from separate groups of animals. To fully appreciate the acute effects of DHA along the entire rostro-caudal spinal cord axis, the expression of CD16/32 and arginase-1 was analysed in sequential 3 mm rostro-caudal segments of contused rat spinal cord at 3 days post-injury (Figure 4A). Both markers were detected in the contused tissue, and a significant increase in both CD 16/32 and arginase-1 was observed at the injury epicentre (in comparison to □□III tubulin control protein) after DHA treatment (Figure 4B-F).

Furthermore, to investigate whether an increase in CD16/32 and arginase-1 expression is also detected in another model of SCI, we studied a lateral hemisection model in mice using immunohistochemistry. In the lateral hemisection mouse model at 7 day post injury, there was limited CD16/32 (M1 phenotype) expression level, but high arginase-1 (M2 phenoptype) expression level that was confined to the ipsilateral side of the injury (Suppl. Figure 1). In comparison to the vehicle group, at 35 days post-contusion in mice, markers for both phenotypes were detected. Treatment with DHA significantly increased the number of CD16/32 immunopositive cells at the injury epicentre in the gray matter (Figure 4G-I), and immediately caudal to the injury epicentre in the white matter (Figure 4J). Similarly, in comparison to the vehicle group at 35 days post-contusion in mice, treatment with DHA significantly increased the number of arginase-1 immunopositive cells at the injury epicentre and immediately caudal to the epicentre in the gray matter (Figure 4K-M), as well as at the injury epicentre within white matter (Figure 4N). These results suggest that DHA is able to enhance the M1 and M2 phenotypes at the acute and chronic stages of spinal cord contusion injury, in the two species.

DHA reduces the M1 phenotype in peripheral primary murine bone marrow-derived macrophages, but not the phagocytic activity

To characterize the effect of DHA on microglia and monocyte-derived macrophages originating in the periphery, we first tested primary murine bone marrow-derived macrophages, which were used to investigate the effect of DHA on the peripherally originating macrophage population. The concentration of DHA used was similar to that previously used in other primary cultures studies (25). DHA at 1 and 3 μM did not significantly alter the number of non-activated (M0) or M2 macrophages (Figure 5A-I). However, DHA at 3 μM significantly reduced the number of M1 macrophages (Figure 5A-H).These results suggest that DHA can significantly reduce the M1 phenotype, but not the M0 and M2 phenotypes of peripheral monocyte-derived macrophages. In an additional experiment, the effect of DHA on the phagocytic activation of M1 or M2 macrophages was studied. No significant change was observed between the DHA-treated group at 3 □M, compared to the vehicle control group (Figure 5J-R). Therefore, the observed modulatory effects of DHA on M1/M2 markers in the spinal cord after injury are unlikely to involve peripherally originating macrophages.

DHA increases miR-124 in microglia and reduces phagocytosis of myelin in vivo

Since microglia have phagocytic activity in the CNS (5, 33), the significant increase in activated microglia by DHA could result in increased phagocytosis and improved debris clearance. To test this hypothesis, the levels of myelin co-localised within microglia/macrophages were analysed using immunohistochemistry. At the injury epicentre level, there was a high level of myelin present within Iba1-positive cells of vehicle- and DHA-treated rats, at 7 days post- contusion (Figure 6A-F). However, to our surprise, the level of myelin present within Iba1-positive cells at 4 and 6 mm rostral to the injury epicentre in DHA-treated rats was significantly reduced compared to vehicle-

treated rats (Figure 6G-M). To further understand how DHA may alter microglial function, we studied a particular microRNA, miR-124, which has been shown to have an important association with microglia/macrophage activation. Thus, miR-124 has been previously shown to correlate inversely with microglia/macrophage activation, as well as inducing the M2 neuroprotective phenotype (34, 35).Using the fluorescent in situ hybridisation (FISH) technique, we show that there was a significant increase in miR-124 expression in the Iba1-positive microglia/macrophages of DHA-treated compared to vehicle-treated SCI animals at 7 days post-injury in contused rats (Figure. 7A-G).

To investigate how these changes are associated with neurological outcome, we studied the phagocytosis of myelin in mouse contusion SCI. Recently, the *P2RY12* gene (purinergic receptor P2Y12) has been found uniquely in microglia and not monocyte-derived macrophages (6, 36, 37). Therefore, the co-expression of P2Y12 and myelin-binding protein (MBP) as a myelin marker was analysed in microglial cells in vehicle- and DHA-treated mice, at 7 days post-contusion, and the neurological outcome was assessed in parallel (Fig. 8A-K). In the rostral and caudal regions, there was a significant reduction in the MBP staining within P2RY12-positive cells, after administration of DHA (Fig. 8B-K). These observations in both contused rats and mice suggest that the phagocytic property of microglia is reduced by DHA. Furthermore, we also showed a significant increase in miR-124 expression in P2Y12 positive microglia of DHA-treated compared to vehicle-treated SCI mice at 7 days post injury (Fig. 9). Importantly, intraspinal administration of a miR-124 inhibitor significantly reduced the miR-124 levels (Fig. 9) and prevented the reduced phagocytic response of microglia, and this was parallel with the compromised neurological recovery (Figure 8). This suggests that the reduced phagocytic activity of microglia is associated

with an increase in miR-124 expression within microglia. Interfering with this modulation of miR-124 activity appears to have a major impact on the beneficial effects of DHA.

DHA acts via miR-124 to reduce microglial phagocytosis of myelin in cultures

To further provide evidence that DHA can reduce the phagocytic response of microglia, DHA was added to primary adult spinal microglia cultures which were exposed to myelin stained with the fluorescence dye DiI, to observe phagocytic effects. In the presence of DHA (1 and 3 μM), there was a general reduction in DiI-labelled myelin detected within adult primary microglia, with a significant reduction observed at 1 μM DHA at 24 hours after incubation, as detected using fluorescent microscopy (Figure 10A-G). To determine if DHA directly influences microglia via miR-124, the microglial miR-124 expression was analysed using quantitative RT-PCR. MiR-124 expression was significantly increased in the DHA-treated primary adult microglia cultures, specifically at 1 μM, when compared to the control group (Figure 10H). To test whether the effect seen is specific to miR-124, another microRNA that modulates the microglia immune response, miR-155, was also investigated (38). Interestingly, no significant difference was observed in miR-155 expression at any of the DHA concentrations studied (Figure 10I). To further test the effect of DHA on the phagocytic ability of microglia, the commonly used BV2 microglial cells were also studied. DHA at 3 μM caused a significant reduction in the amount of DiI-myelin present within the BV2 cells (Figure 10J-K, M). In addition, inhibition of miR-124 using a miR-124 inhibitor (3 pmol/ml) was able to significantly reverse the ability of DHA to suppress myelin phagocytosis by BV2 cells (Figure 10L-M). These results further suggest that the phagocytic property of microglia is reduced by DHA, and this is dependent on changes in miR-124.

DHA reduces phagoptosis of UV-stressed neurones by microglia

In recent studies, activated microglia have been shown to phagocytose stressed but viable neurons, alongside lesion debris and dead cells (9). Therefore, DHA may confer neuroprotection by preventing phagoptosis (the phagocytosis of stressed but viable cells), thus providing time for neurons to self-repair or recover. To test this hypothesis, UV-stressed PC12 neurons were incubated with DHA-treated BV2 microglial cells. PC12 neurons were exposed to 200 mJ/cm^2 and then left for 16 h, which caused a significant increase in apoptosis as detected by labelling for phosphatidylserine (using Annexin V; Suppl. Figure 2A-C). UV-stressed PC12 cells were then labelled with TMRE (red) and Hoechst (blue), a live mitochondria marker and nucleus stain, respectively. The use of TMRE and Hoechst enabled the visualisation of live stressed PC12 cells (red and blue). Of note, when live stressed (apoptotic) PC12 cells come into contact with BV2 microglia, the Hoechst (blue) staining remains, whereas the red colour from TMRE is no longer present. In addition, the BV2 microglia were labelled with CMFDA (green) when co-cultured with neurons.

Using live imaging microscopy, we show that BV2 microglia induce a TMRE loss (mean ± S.E.M.) of 63.7 ± 2.9 % in UV-stressed PC12 cells (Figure 11A & C). However, when BV2 microglia were pre-treated with DHA, there was a marked and significant reduction in the number of cells with TMRE loss, of 32.8 ± 11.5 and 28.5 ± 9.2, at the 1 or 3 μM DHA concentrations, respectively (Figure 11A-C).These results suggest that DHA reduces the phagoptotic effect of microglia, thus providing one of the potential mechanisms enhancing the survival of viable stressed neurons.

Discussion

The present study demonstrates that DHA promotes significant functional improvement as well as neuroprotection after spinal cord trauma in two rodent contusion injury models – and this consolidates the neuroprotective profile shown for this fatty acid in hemisection and compression models, thus enhancing the clinical translation potential. The neuroprotective benefits of DHA are associated with an increase in activated microglia/macrophages at the injury epicentre, both for the M1 and M2 phenotype. In a model of peripheral monocyte-derived macrophages, DHA promoted only a reduction in the M1 phenotype of bone marrow-derived macrophages and had no significant effect on either the M0 or M2 phenotypes. In vivo, DHA promoted an increase in microglial miR-124 expression, with reduced phagocytosis of myelin at 7 days post contusion. In vitro, DHA promoted a reduction in the phagocytosis of myelin by two types of microglial cell cultures. Furthermore, DHA prevented the microglial phagoptosis of stressed but viable neurons. The reduction in the myelin phagocytic response in vitro was linked to a DHA-induced increase in miR-124, and not miR-155.

DHA improves neurological outcome and protects neurones after contusion SCI

A number of studies have examined the neuroprotective effects of omega-3 fatty acids following SCI induced by hemisection or compression (22, 24, 25, 27, 29, 39). So far, several favourable effects of DHA administration (behavioural and histological) post-injury have been described, including decreased axonal and myelin damage, increased neuronal and oligodendrocyte survival, decreased macrophage/microglia cell recruitment and reduced lipid peroxidation and COX-2 activation (22, 24, 25, 27, 29, 39, 40). The results of the current study show that DHA treatment

30 minutes post-injury significantly improves locomotor function in rodents, both in the early (7 days) and late phase (35 days) of spinal cord contusion injury. As transection or hemisection injuries are rarely seen in human spinal cord trauma, contusion injuries are a more relevant model for investigating the potential of various new treatments for human SCI (30, 41, 42). We have previously demonstrated that DHA can improve neurological outcomes in contusion-injured rats in the first week after injury (31), and we further demonstrate in the present study that significant locomotor improvement continues to 28 and 35 days post-injury in rats and mice, respectively, therefore the beneficial effect is robust and persistent. In accordance with improved motor recovery, increased neuronal survival was also observed at 7 and 28 days post-contusion in DHA-treated rats. Furthermore, DHA-treated mice also showed significantly improved neuronal survival when compared to vehicle-treated animals at 35 days post contusion. Thus, the demonstration of significant locomotor recovery alongside improved neuronal survival after contusion injury supports a considerable neuroprotective role for DHA, acutely administered post-SCI.

However, the observations reported so far in SCI have not differentiated the impact of this fatty acid on different microglia/macrophage cell populations and phenotypes, and this was a major focus of the present study. First, we showed that DHA treatment significantly increased Iba-1 expression levels during the early phase (7 days) of contusion SCI in rats. Overall, Iba-1 immunopositive microglia/macrophage cell counts were either unaffected or decreased by DHA treatment during the late phase of contusion SCI in rats and mice (28 and 35 days). As activated microglia/macrophages have been shown to acquire an alternative M2 polarised phenotype (identified by $CD206^{+}$/$CD204^{+}$/arg-1^{+}) during the early phases of SCI (3, 21), by enhancing the

M2 response DHA could provide additional neuroprotective support. Later on, as microglia/macrophages are said to drift towards a predominantly M1 polarised phenotype (identified by $CD16^+/CD32^+/CD86^+/iNOS\text{-}1^+$) during the post-acute and chronic phases of SCI (3, 21), DHA treatment may also potentially dampen harmful cell phenotypes over time.

Pre-stimulated macrophages implanted into damaged rodent spinal cords greatly improve functional recovery after injury (15, 43). Taking this complexity into account, DHA treatment has the potential to modulate microglia/macrophage activity in both the early and late phases of SCI, in a manner which may simultaneously enhance beneficial functions and limit deleterious effects of microglia/macrophages. Importantly, we did not find evidence to support the claim that DHA is able to boost only the M2 microglia/macrophage populations after SCI. In fact, our data show an increase in the M1 ($CD16^+/CD32^+$) as well as the M2 ($Arg\text{-}1^+$) population, via Western blot at 3 days and tissue cell counts at 35 days, in mice (Figure 4), strongly suggesting that DHA can augment both M1 and M2 cell phenotypes post- contusion SCI. Although these results did not match our initial hypothesis, we believe two plausible interpretations exist. Firstly, increased M1 populations during the late phase of SCI could represent an earlier DHA-induced expansion of M2 phenotypes, which have subsequently acquired the M1 profile over time. Secondly, the enhancement of M1 microglia/macrophages by DHA-treatment may not necessarily represent per se the acquisition of a neurotoxic phenotype. For example, DHA-treatment of lipopolysaccharide-activated microglia has been shown to inhibit pro-inflammatory mediator release (i.e. NO, iNOS, TNF-α and IL-6) without inducing an alternative anti-inflammatory M2 phenotype (i.e. Arg-1, IL-10) (44). Our results imply that DHA is capable of inducing region-specific M1 responses within both gray and white matter, which might have separate neuroprotective roles. Furthermore, despite

its utility as a working model to study macrophage heterogeneity in vivo, the M1/M2 classification of activated microglia/macrophages is an over-simplification, with at least one additional macrophage activation state, as well as several M2 sub-classifications believed to exist (3, 21, 45, 46). For this reason, it can be assumed that more than one M1 subtype may be present after injury, which, contrary to current views, may serve important neuroprotective functions.

DHA reduces microglial phagocytosis of myelin debris

It is thought that phagocytosis of myelin debris is crucial for lesion clearance and subsequent axonal repair (47). Recently, Chen and colleagues showed that DHA and EPA can enhance myelin phagocytosis in vitro (48). To our surprise, in our study DHA did not enhance phagocytosis of myelin debris in primary adult microglia cultures; reduced DiI-labelled myelin clearance was observed at 1 μM DHA after 24 hours of incubation (Figure 8). Furthermore, our in vivo data also confirm that DHA treatment causes a reduced phagocytosis of myelin at 7 days after injury (Figure 6). The differences in in vitro results may reflect the fact that Chen and colleagues used primary microglia from neonatal brain and a high DHA concentration (20-80 μM). In contrast with their work, we used primary microglia from the spinal cord of adult animals (which is directly relevant to the microglia population studied in the post-contusion tissue), and in addition a microglia cell line (BV2 cells), and a DHA concentration that was between 1-3 μM, and thus more relevant physiologically. In fact, myelin phagocytosis has been shown to induce the production of many pro-inflammatory mediators (i.e. ROS, TNF-α. IL-6 and IL-1), causing significant bystander damage if left unregulated (49-52). As phagocytosis of myelin has been shown to be neurotoxic in nature and elicit a M1 macrophage response (53), DHA may serve to dampen excessive myelin removal, protecting against further bystander damage. Interestingly, a pro-regenerative treatment

induced by lentiviral vector-driven expression of chondroitinase ABC in contusion SCI, has been shown to lead to an amplification of a phagocytic microglia/macrophage phenotype at 3 days post-injury (Bartus et al., 2014), whereas at 2 weeks after injury the opposite effect was seen. Furthermore, in the same study, a significant amplification of the increase in CD206-expressing microglia triggered by injury, was also seen at 2 weeks after treatment.

When co-cultured with neurons, microglial cells were able to selectively phagocytose and remove dying cells, whilst leaving healthy neurons intact (54). We speculate that the phagocytosis of dying cells by microglia (and possibly also by macrophages) may explain the increased Iba-1 immunopositive expression levels observed at 7 days post-contusion injury. Later on, increases in white matter Iba-1 expression levels and CD16/32 and arginase-1 immunopositive cell counts (epicentre to 1 mm caudal) at 35 days, suggest that DHA may support remyelination in these areas and reduce excessive and unnecessary myelin phagocytosis. Our interpretation is supported by studies on demyelination/remyelination processes (55) which did not find evidence supporting the idea that M1 microglial phenotypes drive demyelination whilst M2 populations enhance remyelination. In fact, the microglia phenotype present during demyelination persists over time post injury, suggesting a gradual and more subtle switch in microglia functions that support remyelination (55). Furthermore, both M1- and M2-phenotype markers were shown to be up-regulated during periods of demyelination and remyelination (55). Microglial cells were also shown to support myelination by providing important trophic support to oligodendrocyte progenitor cells (55). Similarly, concurrent microglial iNOS expression showed moderately protective effects against demyelination (55). Therefore, DHA treatment may be able to prevent

microglia/macrophage cell death after injury, thus enabling the acquisition of more subtle neuroprotective roles of these cells over time.

DHA enhances microglial miRNA-124 expression

To understand how DHA may directly influence microglial cells, the effect of DHA on miR-124 was analysed using FISH and quantitative RT-PCR techniques. Our results indicate that DHA is able to significantly increase microglial miR-124 expression in the injured spinal cord and primary adult microglial culture (Figure 7 & 9). In un-injured spinal cord, miR-124 in microglia was not detectable (data not shown). As miR-124 has been shown to correlate inversely with microglia/macrophage activation, as well as inducing M2 phenotypic changes after CNS trauma (34, 35), our data suggest that DHA is capable of modulating microglial activity after SCI via the enhancement of miR-124 expression. A very important observation in this study is that the early interference with the activity of miR-124, compromises motor improvement after DHA, suggesting that the microglia modulation is an important aspect of the neuroprotective effect of the fatty acid.

Long-chain omega-3 fatty acids such as DHA have a multitude of molecular targets that could drive the effect on miRNA and on microglia activity (56, 57), such as the peroxisome proliferator-activated receptors and retinoid receptors, or TREK-1 channels - targets which are all possible candidates for a modulation of microglia (58, 59), and this aspect remains to be characterised in future studies.

Conclusion

The results of the present study show that DHA can act directly on microglia and reduce their phagocytic activity. DHA induces neuroprotection after moderate or severe contusion SCI in rodents and a markedly improved neurological outcome. Interestingly, DHA seems to be able to enhance early gray matter microglia/macrophage (Iba-1^{+}) cell populations (7 days) when compared to control animals, which then remained unchanged or decreased in the late phase (28 and 35 days) after SCI. Therefore, DHA is able to augment early microglia/macrophage responses after severe contusion. DHA is shown to enhance gray and white matter M1 (CD16/32^{+}) responses in mouse contused cords at 35 days. Increased M1 populations may represent an earlier DHA-induced expansion of M2 phenotypes that have subsequently acquired M1 reactivity over time, or the acquisition of a non-reactive M1 phenotype, enabling improved locomotor recovery. Furthermore, increased white matter CD16/32^{+} microglia/macrophage populations over time may enhance remyelination and support oligodendrocyte cells in this process. DHA-treatment reduces myelin phagocytosis in vitro (a process linked to phagoptosis) and enhances miR-124 expression (an important microRNA associated with the acquisition of M2 phenotypes), in vivo and in vitro. Therefore, our data demonstrates that DHA is associated with a complex modulation of the microglia/macrophage response, which occurs in parallel with a significant neuroprotective effect after contusion SCI in rodents.

Materials and Methods

In vivo study

Spinal cord contusion injury

All animal surgery was carried out under the UK Home Office Scientific Procedures Act (1986) and EU directive 2010/63/EU. The ARRIVE guidelines were followed for this study. Female Sprague-Dawley rats (230 - 250 g) were anaesthetized intraperitoneally with a mixture of medetomidine (Domitor, 0.5 mg/kg) and ketamine (Ketaset, 60 mg/kg), after which they received a contusion injury at spinal thoracic level T10/11 level using the PinPoint controlled cortical impactor (velocity; 1.5 m/s, dwell time; 100 ms, penetration depth; 1.7 mm, tip diameter; 2 mm) (Hatteras Instruments, USA). Adult female C57BL6 mice (age 12 weeks old) were anesthetised intraperitoneally with a mixture of medetomidine (0.5 mg/kg) and ketamine (75 mg/kg) before receiving a spinal thoracic level T10/11 contusion injury using the PinPoint controlled cortical impactor (velocity; 0.7 m/s, dwell time; 85 ms, penetration depth; 0.8 mm, tip diameter; 1.5 mm). All animals underwent daily weight monitoring, twice daily buprenorphine treatment and manual bladder expression until it was no longer necessary.

DHA treatment

SCI surgery was performed in two groups of animals receiving either an intravenous (i.v.) injection of vehicle (saline containing 0.2 % ethanol) or DHA (free fatty acid; 500 nmol/kg) (Sigma-Aldrich, D2534) 30 minutes post-injury. All i.v. injections were administered via the tail vein in a volume of 1 ml/kg. Animal surgeons were blinded to treatment type. Sprague-Dawley rats were sacrificed at 7 and 28 days after injury, whereas C57BL6 mice were sacrificed at 35 days after injury.

Intraspinal miR-124 inhibitor and intravenous DHA injection

In a separate study in mice with contusion SCI, animals received 0.5 μl intraspinal injections in both the caudal and rostral region of the contused spinal cord using a glass micro glass needle via a microinfusion pump, as previously described (27, 60). Each mouse received either 25 pmol of miR-124 miRCURY LNA miRNA inhibitor or negative control A, which acts as a miRCURY LNA miRNA inhibitor control (Exiqon, Y104101112, Y100199006) mixed with Lipofectamine 2000 (Invitrogen, 2 μl in 50 μl PBS) as the transfection reagent. Thirty minutes post contusion injury, DHA or vehicle were intravenously administered as described above.

Behavioural analysis

The Basso-Beattie-Bresnahan (BBB) open field locomotor rating score (0-21) and Basso Mouse Scale (BMS) (0-9) were used to rate hind limb movement following contusion (61, 62). BBB and BMS scoring was conducted in an open field (4 minute sessions) on days 1-7, 14 and 28 post-injury (Sprague-Dawley rats), as well as every day for the first week, then every other day until 35 days post-injury (C57BL/6 mice). All tests were performed and analysed by individuals who were blinded to the treatment type.

Immunohistochemistry

Animals were perfused with saline followed by 4% paraformaldehyde, for histology. Spinal cord segments containing the lesion site including the rostral and caudal regions were dissected out and embedded in OCT compound. Serial horizontal cryostat sections (rat; 20 μm, mice; 15 μm) were collected across SuperFrost Plus microscopes slides and processed for immunohistochemistry. Each slide contained a selection of dorsal, intermediate and ventral cord sections. Sections

underwent 3 x 5 min 10 mM phosphate buffer saline (PBS) washes before incubation in 0.3 % hydrogen peroxide in PBS for 10 min to remove endogenous peroxidase. For all washes, sections were gently agitated on a shaker. For immunohistochemical labelling, sections were blocked with 10 % normal goat serum (containing 10 mM PBS, Triton X-100 and sodium azide) for 1 hour before incubation with the primary antibody. Antibodies used were: ionised calcium binding adaptor molecule 1 (Iba-1, 1:1000, Wako 019-19741), which labels activated and non-activated microglia/macrophages; P2Y12 (1:200, Cambridge Bioscience, ANA55043A), which labels microglia; CD16/32 (1:500, BD Pharmingen 553141), a specific marker of M1 activated microglia/macrophages; Arginase-1 (1:250, Santa Cruz, sc-18354), a specific marker of M2 activated microglia/macrophages, NeuN (1:1000, Chemicon MAB377), for neuronal cells; myelin basic protein (MBP, 1:500, Abcam ab62631) for the most abundant protein component of myelin. Sections were incubated with primary antibody overnight in a humidified chamber at room temperature. The following day, sections underwent 3 x 5 min PBS washes before incubation with secondary Alexa Fluor antibodies (Invitrogen®). Tissue sections were incubated in a humidified chamber for 2 hours at 4°C. After application of secondary antibodies, sections underwent a further 3 x 5 min PBS washes before mounting with Vectashield and DAPI.

Fluorescence In situ hybridisation (FISH) and Immunohistochemistry

The FISH procedure was carried out using the 5'-biotin labelled rno-miR-124 microRNA in situ probe (miRCURY LNA™ detection probe, Cat. No. 614870-370, Exiqon) according to manufacturer's instructions similarly to previously published (63). Briefly, horizontal rat spinal cord sections containing the injury site were washed 3 x 5 min DEPC-treated 10 mM PBS then dehydrated through a graded series of alcohol and air-dried. Sections were incubated overnight

with 40 nM miR-124 microRNA probe diluted with microRNA in situ hybridisation buffer (Cat No. 90004, Exiqon) at 59 ^{o}C. RNase A-treated spinal cord sections were used as a negative FISH control. Next day, slides were washed in a series of pre-heated DEPC-saline-sodium citrate (SSC) solutions at 59^{o}C for 5 min each. After further washes in 0.2 x SSC and 1 x PBS at room temperature for 5 min each, slides were incubated with 0.3% hydrogen peroxide for 30 min. Thereafter, the biotin signal on the miR-124 microRNA was amplified using the Avidin-Biotin complex (Vectastain ABC Elite Kit, Vector Labs) and biotinyl tyramide (1:75, NEN Life Science Products), and visualised with ExtrAvidin®-FITC (1:400, Sigma). After the FISH procedure, the sections were incubated with Iba1 antibody overnight followed by secondary Alexa Fluor 594 for 2 h, and coverslipped with Vectashield and DAPI as mentioned above.

Image Analysis

Spinal cord sections with NeuN, Iba-1, CD16/32, Arg-1 and MBP immunolabelling, and miR-124 FISH staining were viewed on a Leica epifluorescence microscope. Images were obtained using a 20x objective lens. In rat spinal cord tissue sections, two adjacent regions of interest (ROI) were selected for analysis at the contusion epicentre as well as regions rostral and caudal to the injury epicenter (2, 4 and 6 mm rostral and caudal). Images of each ROI were captured at 3 different depths (dorsal, central and ventral sections of the cord). For rat contused cords, the area occupied by Iba-1 immunopositive cells was measured using the MetaMorph image analysis programme. Percentage threshold area (area occupied by immunopositive cells) was calculated via the use of intensity thresholding. Co-localisation of Iba1^{+} cells with MBP or miR-124 was analysed using ImageJ. For mice contused cords, immunopositive cell number and size were recorded every 1 mm in the rostrocaudal plane and at 3 different depths, using the Image J software programme.

Cell counts and cell size were averaged per ROI and then per whole cord to give overall values for the lesion epicentre as well as ROI rostrally and caudally. For the localisation of myelin within microglia, a customised macro was used to identify the co- localisation of myelin within Iba1+ cells in the white matter from 7d contused rat spinal cord. The difference in some of the image analysis used between different experiments was due to the studies being carried out simultaneously and independently by different members of the research group. For the identification of myelin within P2Y12+ microglial cells in the spinal cord of 7d contused mice, a customised ImageJ macro was used. A 500 μm x 500 μm square was placed within the ROI of each side of the spinal cord. The macro enabled all P2Y12+ staining within the ROI of the image and all the MBP staining within the ROI of the same image to be identified. Thereafter, the images were superimposed and only MBP staining present within the P2Y12+ cells was considered for the quantification. The MBP staining value for each ROI was the average MBP staining per P2Y12+ microglial cell.

Western blot analysis

The method used has been previously described (64). Briefly, adult rats with spinal cord contusion injury were either treated with DHA or vehicle at 30 min post contusion as mentioned above. Three days post injury, the animals were sacrificed and the spinal cord was quickly removed onto dry ice and then stored at -80^{o}C until further processing. The spinal cord was dissected into 3 mm thick cross sections, with the centre of the injury site as the epicentre. A further 2 and 3 segments were also removed caudal and rostral to the epicentre, respectively. The protein from each cord segment was harvested in 1 ml ice-cold lysis buffer (20 mM HEPES pH 7.4, 100 nM NaCl, 100 mM NaF, 1 mM Na_2VO_4, 5 mM EDTA, 1% Nonidet P-40 and 1X protease inhibitor cocktail; Roche). The

homogenate was rotated for 2 h at 4ºC before centrifugation at 13,500 g for 15 min at 4ºC. The total protein concentration of the supernatant was determined using the bicinchoninic acid protein (BCA) assay kit (Pierce).

Fifteen micrograms of total protein were electrophoresed on 12% acrylamide gel before transfer onto Hybond P membranes and incubated overnight at room temperature with rat anti-CD16/32, rabbit anti-arginase-1, or mouse anti-βIII tubulin (control protein). To avoid batch differences, each blot contained an animal from each treatment group.

In vitro study

Bone marrow derived macrophages

The method used has been previously described (21). Briefly, the tibias and femurs of C57BL/6 mice were removed and the bone marrow flushed out using RPMI 1640 with 10% fetal bovine serum. Cells were triturated 3-5 times and red blood cells lysed in lysis buffer (0.15M NH_4Cl, 10 mM $KHCO_3$, 0.1 mM Na_2EDTA; pH7.4). After a single wash in media, cells were cultured in RPMI 1640 containing 1% penicillin/streptomycin, 1% HEPES, 0.001% β-mercaptoethanol, 10% FBS and 20% supernatant from sL929 cells. After 7-10 days, when the bone marrow cells have differentiated into macrophages, the cells were either treated with media alone (termed M0) or differentiated into M1 or M2 macrophages. The differentiation into M1 macrophages required treatment with LPS (100 ng/ml) and IFN-γ (20 ng/ml). The differentiation into M2 macrophages required treatment with IL-4 (20 ng/ml). After 30 min of either control or treatment to differentiate into M1 or M2, DHA (1-3 μM) was incubated with the macrophages. Twenty-four hours later, the cells were fixed with 4% paraformaldehyde and underwent immunostaining for Iba1, CD16/32 and DAPI.

The number of cells and immunostaining intensity was measured using the Thermo Scientific™ ArrayScan™ XTI High Content Analysis Reader. Ten regions of each well with each treatment and condition consisting of two wells were analysed. Four independent experiments were carried out.

Primary adult rat microglia culture

Primary microglia cultures from adult rat spinal cord were carried out as previously described (65). Briefly, adult Wistar rats were deeply anaesthetised with sodium pentobarbital (120 mg/kg, i.p.) then perfused with saline to flush away monocytes/macrophages. The spinal cord was dissected out and placed into ice-cold Hanks Balanced Salt Solution (HBSS) media. The dura mater and spinal roots were removed before cutting longitudinally at 200 µm segments using a McIlwain tissue chopper. After digestion in papain followed by dissociation, the cell suspension was passed through a 70 µm sieve. Five µl of cell suspension was stained with 5 µl DAPI. Using an epi-fluorescent microscope DAPI immunopositive cells were counted and 40,000 cells were plated into each well containing a sterile ethanol-cleaned 13 mm diameter cover slip. After 2 h, un-attached cells were washed away with DFP media (containing Dulbecco's modified eagle medium (DMEM), 15% heat-inactivated foetal bovine serum (HI-FBS) and penicillin-streptomycin; 100 IU/ml), and allowed to incubate overnight at 37^{o}C and 5% CO_2 and were used the next following day for experimental studies.

For data analysis, Iba-1 and DiI immunopositive cells were counted using the Image J program. Ten regions of interest were selected for analysis per well (65). The average amount of DiI within

each cell per DHA treatment concentration was analysed. Four independent experiments in each treatment group; control (DFP media containing 0.0003% ethanol), 1 and 3 µM DHA were studied.

Retroviral immortalised murine (BV2) microglia culture

The BV2 microglia cell line was cultured as previously described (66). Briefly, BV2 cells were cultured in DMEM supplemented with 10 % HI-FBS and penicillin-streptomycin under 37 ^{o}C and 5 % CO_2. During experimental studies, the HI-FBS was reduced to 5 %.

Myelin phagocytosis

Preparation of spinal cord myelin

Myelin was purified from rat spinal cord tissue by sucrose gradient centrifugation as previously described (67, 68). Briefly, the spinal cords were homogenised with a glass-glass homogeniser in 0.32 M sucrose and then layered onto 0.85 M sucrose. After centrifugation at 75,000 g for 30 min, the crude myelin was transferred into 20 volumes of 0.32 M sucrose and centrifuged 13,000 g for 25 min. The white myelin pellet was resuspended in 25 volumes of sterile water and centrifuged at 15,000 g for 25 min. The pure myelin pellet was dissolved in 2.5 mM Tris (pH 7.0) and the protein concentration was determined using the Pierce BCA assay.

DiI labelling of myelin

Labelling of spinal cord myelin with fluorescent dye DiI was carried out as previously described (69). Myelin (1 mg/ml) was labelled by incubating with DiI (0.2 mg/ml, Cambridge Bioscience Ltd, BT60010) at 37^{o}C for 30 min. After resuspension with 40 volumes of sterile DPBS, the

solution was briefly sonicated for 15 s to decrease particle size (70). After centrifugation at 15,000 g for 5 min, the DiI-labelled myelin was resuspended in 5 % DMEM (1 mg/ml).

Phagocytosis of DiI-myelin

Microglia or bone marrow-derived macrophages were incubated for 30 min with DiI-labelled myelin (50 μg) per well before DHA (1-3 μM) was added. After 24 h, the media were removed and the cells were either frozen on dry ice for RNA extraction or fixed with 4% paraformaldehyde for immunocytochemistry.

Inhibition of DiI-myelin phagocytosis in vitro

To study the role of DHA on miR-124, 3 pmol/ml miRCURY LNA microRNA inhibitor specifically designed for rno-miR-124 (Exiqon, 4104239-001) complexed with the transfection reagent Lipofectamine 2000 (Invitrogen) was added an hour before application of DHA, as previously described (25).

Phagoptosis of UV stressed neurones

Neuronal (PC12) cell lines were used to assay the effect of DHA on the phagoptosis of microglia BV2 cells similarly to the method previously published (9).

PC12 cells

PC12 cells were cultured in complete medium (containing DMEM, 5% heat inactivated horse serum, 5% HI-FBS and penicillin-streptomycin) at 37^{o}C and 5% CO_2. During the experimental studies, the PC12 cells were transferred onto collagen (2 mg/ml, Roche Diagnostics,

11179179001) covered 9 cm dish HI-FBS and were differentiated into neurons when cultured in differentiation medium (containing DMEM, 1% heat-inactivated horse serum, nerve growth factor (50 ng/ml, Sigma-Aldrich, N0513), and penicillin-streptomycin).

Live cell imaging

On the day of the experiment, BV2 and PC12 cells were incubated with the relevant fluorescent dyes for 20 min at 37 ^{o}C and 5 % CO_2, and then thoroughly washed several times with DPBS to remove any free dye. BV2 cells were labelled with 5-chloromethylfluorescein diacetate (0.4 □M, CellTracker^{TM} green CMFDA, C7025, a green fluorescent dye suited for monitoring cellular movement and location). PC12 cells were exposed to 200 mJ/cm^2 irradiation using the CX-2000 UV crosslinker to stress the neuronal cells. The following day, the UV-treated PC12 cells were stained with tetramethylrhodamine ethyl ester (25 nM, TMRE, ThermoFisher, T-669, a red fluorescence dye that readily labels active mitochondria) and Hoechst 33342 (10 μg/ml, ThermoFisher, H1399, a blue fluorescence dye that is a cell-permanent nuclear counterstain). Sixteen hours after the UV treatment, the PC12 cells were harvested by trypsinisation and added onto the DHA-treated BV2 cells. Time-lapse microscopy was conducted on an inverted microscope (Zeiss Axiovert 200M) at x20 magnification in improved MEM (ThermoFisher, 10373-017) without Phenol red, supplemented with 5 % HI-FBS and using the 24 well plate at 37 ^{o}C, 5% CO_2 and in a humidity-controlled chamber. Two regions within the well were randomly selected and images were time-lapse captured every 9 min for a total of 3 h.

Analysis of time-lapse microscopy

The number of contacts made between a BV2 cell (green) and UV-stressed PC12 cells (red with blue nuclei) was recorded. After the contact was made, the number of PC12 cells which lost the red fluorescence as an indicator of no active mitochondria was also recorded.

UV-induced apoptosis

To confirm that neuronal PC12 cells were stressed from the UV irradiation protocol, PC12 cells plated onto collagen-coated glass coverslips and cultured in differentiation medium were exposed to 200 mJ/cm^2 irradiation. Sixteen hours after the UV treatment, the PC12 cells were stained using Annexin V Alexa Fluor® 488 (ThermoFisher, V13241) according to the manufacturer's instruction for imaging microscopy.

Immunocytochemistry

All microglial cultures underwent 3 x 5 min PBS washes before incubation with primary antibodies for two hours. Primary microglia were stained using rabbit anti-Iba1 (1:500 Wako) and BV2 microglia cell lines were stained with biotinylated Isolectin-B4 (1:200, Vector Labs B-1205) before applying secondary antibodies for 45 minutes. After performing 3 further PBS washes, microglia cultures on glass cover slips were mounted onto glass slides with DAPI and Fluorsave mounting media. The lipophilic dye DiI was used to visualise myelin within microglial cultures, which is a red fluorescence dye when viewed with fluorescent microscopy.

Quantitative RT-PCR analysis of miRNA

Total RNA was extracted from primary adult microglia cultures by using the miRVANA™ PARIS™ isolation kit (AM1560, Life technologies) similarly to previously published (71). Microglial cells from 2 wells per treatment were pooled together. Total RNA was quantified using the ND1000 spectrophotometer (NanoDrop Technologies, UK). Analysis of miR-124 expression was carried out using the TaqMan miRNA assays (Assay ID: 001182) and performed on Applied Biosystems 7500 Real Time PCR system. The internal control used was RNU6B (Assay ID: 001093). Quantitative RT-PCR analysis was performed in triplicates from four independent experiments.

Statistical analysis

All statistical analysis of results was carried out using the GraphPad Prism program. For behavioural data, and staining for NeuN, Iba-1, CD16/32, Arg-1, MBP, and miR-124, a two way repeated measures ANOVA was used to compare the overall effect of DHA and vehicle injection. Individual differences between DHA- and vehicle-treated animals were determined using Tukey's post-hoc tests. For DHA-treated microglial cultures and quantitative RT-PCR analysis of miRNA, a one-way repeated measures ANOVA was used to compare DHA versus control groups. Individual differences between DHA concentrations were determined using Dunnett's post-hoc tests. Statistical significance was set at $p<0.05$. Data points are represented as the mean +/- standard error of the mean (SEM).

For the in vitro experiments, 10 regions of each well, with each treatment and condition consisting of two wells were analysed. Three or four independent experiments were carried out. The number of cells and immunostaining intensity from the BMDM experiment was measured using the Thermo Scientific™ ArrayScan™ XTI High Content Analysis Reader. The statistical analysis used was one way ANOVA followed by Tukey's post-hoc test. Statistical significance was set at $p<0.05$. Data points are represented as the mean +/- standard error of the mean (SEM).

Acknowledgements

The authors would like to thank Dr Kristina Kigerl for help with Thermo Scientific™ ArrayScan™ XTI High Content Analysis Reader, Dr Jan Stoetaert and Dr Belén Martín-Martín of the BALM facility for help with time-lapse microscopy and Dr Xuenong Bo for the supply of PC12 cells.

This study was supported by the US Department of Defence CDMRP/SCIRP award (Reference W81XWH-10-1-1040) (PKY, TB, AMT), The Barts and London Charity (PKY, AMT), Rod Flower Vacation Scholarship (ALB), International Spinal Research Trust (JH, PGP), Ray W. Poppleton Endowment (PGP) and Chang Gung Memorial Hospital, Taiwan CMRPG3A1051–1054 (Z-HL).

Contributions

The authors(s) have made the following declarations about their contributions: Conceived and designed the experiments: PKY, PGP, AMT. Performed the experiments and analysed the data: PKY, ALB, MB, TB, ZHL, MAKEM, FG, ADL, SURN, JH. PKY, AMY, ZHL, FG, ADL, SURN. Contributed reagents/materials/analysis tools: PKY, PGP, AMT. Wrote the paper: PKY, ALB, PGP, JCEH, JVP, AMT.

Conflict of Interest

The authors declare that there is no conflict of interest regarding the publication of this article.

References

1 van den Berg, M.E., Castellote, J.M., de Pedro-Cuesta, J. and Mahillo-Fernandez, I. (2010) Survival after spinal cord injury: a systematic review. *Journal of neurotrauma*, **27**, 1517-1528.

2 Bowes, A.L. and Yip, P.K. (2014) Modulating inflammatory cell responses to spinal cord injury: all in good time. *Journal of neurotrauma*, **31**, 1753-1766.

3 David, S. and Kroner, A. (2011) Repertoire of microglial and macrophage responses after spinal cord injury. *Nature reviews. Neuroscience*, **12**, 388-399.

4 Popovich, P.G., Guan, Z., McGaughy, V., Fisher, L., Hickey, W.F. and Basso, D.M. (2002) The neuropathological and behavioral consequences of intraspinal microglial/macrophage activation. *J. Neuropathol. Exp. Neurol.*, **61**, 623-633.

5 Town, T., Nikolic, V. and Tan, J. (2005) The microglial "activation" continuum: from innate to adaptive responses. *J. Neuroinflammation*, **2**, 24.

6 Butovsky, O., Jedrychowski, M.P., Moore, C.S., Cialic, R., Lanser, A.J., Gabriely, G., Koeglsperger, T., Dake, B., Wu, P.M., Doykan, C.E. *et al.* (2014) Identification of a unique TGF-beta-dependent molecular and functional signature in microglia. *Nature neuroscience*, **17**, 131-143.

7 Brown, G.C. and Neher, J.J. (2012) Eaten alive! Cell death by primary phagocytosis: 'phagoptosis'. *Trends Biochem. Sci.*, **37**, 325-332.

8 Brown, G.C. and Neher, J.J. (2014) Microglial phagocytosis of live neurons. *Nature reviews. Neuroscience*, **15**, 209-216.

9 Fricker, M., Oliva-Martin, M.J. and Brown, G.C. (2012) Primary phagocytosis of viable neurons by microglia activated with LPS or Abeta is dependent on calreticulin/LRP phagocytic signalling. *J. Neuroinflammation*, **9**, 196.

10 Bessis, A., Bechade, C., Bernard, D. and Roumier, A. (2007) Microglial control of neuronal death and synaptic properties. *Glia*, **55**, 233-238.

11 Polazzi, E. and Monti, B. (2010) Microglia and neuroprotection: from in vitro studies to therapeutic applications. *Progress in neurobiology*, **92**, 293-315.

12 Aloisi, F., Ria, F., Penna, G. and Adorini, L. (1998) Microglia are more efficient than astrocytes in antigen processing and in Th1 but not Th2 cell activation. *J. Immunol.*, **160**, 4671-4680.

13 Popovich, P.G., Guan, Z., Wei, P., Huitinga, I., van Rooijen, N. and Stokes, B.T. (1999) Depletion of hematogenous macrophages promotes partial hindlimb recovery and neuroanatomical repair after experimental spinal cord injury. *Experimental neurology*, **158**, 351-365.

14 Saville, L.R., Pospisil, C.H., Mawhinney, L.A., Bao, F., Simedrea, F.C., Peters, A.A., O'Connell, P.J., Weaver, L.C. and Dekaban, G.A. (2004) A monoclonal antibody to CD11d reduces the inflammatory infiltrate into the injured spinal cord: a potential neuroprotective treatment. *J. Neuroimmunol.*, **156**, 42-57.

15 Rapalino, O., Lazarov-Spiegler, O., Agranov, E., Velan, G.J., Yoles, E., Fraidakis, M., Solomon, A., Gepstein, R., Katz, A., Belkin, M. *et al.* (1998) Implantation of stimulated homologous macrophages results in partial recovery of paraplegic rats. *Nat. Med.*, **4**, 814-821.

16 Schwartz, M., Moalem, G., Leibowitz-Amit, R. and Cohen, I.R. (1999) Innate and adaptive immune responses can be beneficial for CNS repair. *Trends Neurosci.*, **22**, 295-299.

17 Ding, A.H., Nathan, C.F. and Stuehr, D.J. (1988) Release of reactive nitrogen intermediates and reactive oxygen intermediates from mouse peritoneal macrophages. Comparison of activating cytokines and evidence for independent production. *J. Immunol.*, **141**, 2407-2412.

18 Gordon, S. and Taylor, P.R. (2005) Monocyte and macrophage heterogeneity. *Nat. Rev. Immunol.*, **5**, 953-964.

19 Martinez, F.O., Helming, L. and Gordon, S. (2009) Alternative activation of macrophages: an immunologic functional perspective. *Annu. Rev. Immunol.*, **27**, 451-483.

20 Sica, A., Schioppa, T., Mantovani, A. and Allavena, P. (2006) Tumour-associated macrophages are a distinct M2 polarised population promoting tumour progression: potential targets of anti-cancer therapy. *Eur. J. Cancer*, **42**, 717-727.

21 Kigerl, K.A., Gensel, J.C., Ankeny, D.P., Alexander, J.K., Donnelly, D.J. and Popovich, P.G. (2009) Identification of two distinct macrophage subsets with divergent effects causing either neurotoxicity or regeneration in the injured mouse spinal cord. *The Journal of neuroscience: the official journal of the Society for Neuroscience*, **29**, 13435-13444.

22 Huang, W.L., King, V.R., Curran, O.E., Dyall, S.C., Ward, R.E., Lal, N., Priestley, J.V. and Michael-Titus, A.T. (2007) A combination of intravenous and dietary docosahexaenoic acid

significantly improves outcome after spinal cord injury. *Brain : a journal of neurology*, **130**, 3004-3019.

23 Lim, S.N., Gladman, S.J., Dyall, S.C., Patel, U., Virani, N., Kang, J.X., Priestley, J.V. and Michael-Titus, A.T. (2013) Transgenic mice with high endogenous omega-3 fatty acids are protected from spinal cord injury. *Neurobiology of disease*, **51**, 104-112.

24 Lim, S.N., Huang, W., Hall, J.C., Ward, R.E., Priestley, J.V. and Michael-Titus, A.T. (2010) The acute administration of eicosapentaenoic acid is neuroprotective after spinal cord compression injury in rats. *Prostaglandins, leukotrienes, and essential fatty acids*, **83**, 193-201.

25 Liu, Z.H., Yip, P.K., Adams, L., Davies, M., Lee, J.W., Michael, G.J., Priestley, J.V. and Michael-Titus, A.T. (2015) A Single Bolus of Docosahexaenoic Acid Promotes Neuroplastic Changes in the Innervation of Spinal Cord Interneurons and Motor Neurons and Improves Functional Recovery after Spinal Cord Injury. *The Journal of neuroscience : the official journal of the Society for Neuroscience*, **35**, 12733-12752.

26 Pallier, P.N., Poddighe, L., Zbarsky, V., Kostusiak, M., Choudhury, R., Hart, T., Burguillos, M.A., Musbahi, O., Groenendijk, M., Sijben, J.W. *et al.* (2015) A nutrient combination designed to enhance synapse formation and function improves outcome in experimental spinal cord injury. *Neurobiology of disease*, **82**, 504-515.

27 Paterniti, I., Impellizzeri, D., Di Paola, R., Esposito, E., Gladman, S., Yip, P., Priestley, J.V., Michael-Titus, A.T. and Cuzzocrea, S. (2014) Docosahexaenoic acid attenuates the early inflammatory response following spinal cord injury in mice: in-vivo and in-vitro studies. *J Neuroinflammation*, **11**, 6.

28 Hjorth, E. and Freund-Levi, Y. (2012) Immunomodulation of microglia by docosahexaenoic acid and eicosapentaenoic acid. *Curr. Opin. Clin. Nutr. Metab. Care*, **15**, 134-143.

29 Lim, S.N., Huang, W., Hall, J.C., Michael-Titus, A.T. and Priestley, J.V. (2013) Improved outcome after spinal cord compression injury in mice treated with docosahexaenoic acid. *Experimental neurology*, **239**, 13-27.

30 Ek, C.J., Habgood, M.D., Callaway, J.K., Dennis, R., Dziegielewska, K.M., Johansson, P.A., Potter, A., Wheaton, B. and Saunders, N.R. (2010) Spatio-temporal progression of grey and white matter damage following contusion injury in rat spinal cord. *PloS one*, **5**, e12021.

31 Tremoleda, J.L., Thau-Zuchman, O., Davies, M., Foster, J., Khan, I., Vadivelu, K.C., Yip, P.K., Sosabowski, J., Trigg, W. and Michael-Titus, A.T. (2016) In vivo PET imaging of the neuroinflammatory response in rat spinal cord injury using the TSPO tracer [(18)F]GE-180 and effect of docosahexaenoic acid. *Eur. J. Nucl. Med. Mol. Imaging*, **43**, 1710-1722.

32 Hall, J.C., Priestley, J.V., Perry, V.H. and Michael-Titus, A.T. (2012) Docosahexaenoic acid, but not eicosapentaenoic acid, reduces the early inflammatory response following compression spinal cord injury in the rat. *Journal of neurochemistry*, **121**, 738-750.

33 Dheen, S.T., Kaur, C. and Ling, E.A. (2007) Microglial activation and its implications in the brain diseases. *Curr. Med. Chem.*, **14**, 1189-1197.

34 Ponomarev, E.D., Veremeyko, T., Barteneva, N., Krichevsky, A.M. and Weiner, H.L. (2011) MicroRNA-124 promotes microglia quiescence and suppresses EAE by deactivating macrophages via the C/EBP-alpha-PU.1 pathway. *Nat. Med.*, **17**, 64-70.

35 Veremeyko, T., Starossom, S.C., Weiner, H.L. and Ponomarev, E.D. (2012) Detection of microRNAs in microglia by real-time PCR in normal CNS and during neuroinflammation. *Journal of visualized experiments : JoVE*, in press.

36 Bennett, M.L., Bennett, F.C., Liddelow, S.A., Ajami, B., Zamanian, J.L., Fernhoff, N.B., Mulinyawe, S.B., Bohlen, C.J., Adil, A., Tucker, A. *et al.* (2016) New tools for studying microglia in the mouse and human CNS. *Proceedings of the National Academy of Sciences of the United States of America*, **113**, E1738-1746.

37 Haynes, S.E., Hollopeter, G., Yang, G., Kurpius, D., Dailey, M.E., Gan, W.B. and Julius, D. (2006) The P2Y12 receptor regulates microglial activation by extracellular nucleotides. *Nature neuroscience*, **9**, 1512-1519.

38 Cardoso, A.L., Guedes, J.R., Pereira de Almeida, L. and Pedroso de Lima, M.C. (2012) miR-155 modulates microglia-mediated immune response by down-regulating SOCS-1 and promoting cytokine and nitric oxide production. *Immunology*, **135**, 73-88.

39 Ward, R.E., Huang, W., Curran, O.E., Priestley, J.V. and Michael-Titus, A.T. (2010) Docosahexaenoic acid prevents white matter damage after spinal cord injury. *Journal of neurotrauma*, **27**, 1769-1780.

40 Freund-Levi, Y., Hjorth, E., Lindberg, C., Cederholm, T., Faxen-Irving, G., Vedin, I., Palmblad, J., Wahlund, L.O., Schultzberg, M., Basun, H. *et al.* (2009) Effects of omega-3 fatty acids on inflammatory markers in cerebrospinal fluid and plasma in Alzheimer's disease: the OmegAD study. *Dement. Geriatr. Cogn. Disord.*, **27**, 481-490.

41 Hulsebosch, C.E. (2002) Recent advances in pathophysiology and treatment of spinal cord injury. *Adv. Physiol. Educ.*, **26**, 238-255.

42 Mautes, A.E., Weinzierl, M.R., Donovan, F. and Noble, L.J. (2000) Vascular events after spinal cord injury: contribution to secondary pathogenesis. *Physical therapy*, **80**, 673-687.

43 Schwartz, M., Lazarov-Spiegler, O., Rapalino, O., Agranov, I., Velan, G. and Hadani, M. (1999) Potential repair of rat spinal cord injuries using stimulated homologous macrophages. *Neurosurgery*, **44**, 1041-1045; discussion 1045-1046.

44 Antonietta Ajmone-Cat, M., Lavinia Salvatori, M., De Simone, R., Mancini, M., Biagioni, S., Bernardo, A., Cacci, E. and Minghetti, L. (2012) Docosahexaenoic acid modulates inflammatory and antineurogenic functions of activated microglial cells. *J. Neurosci. Res.*, **90**, 575-587.

45 Hanisch, U.K. (2013) Functional diversity of microglia - how heterogeneous are they to begin with? *Frontiers in cellular neuroscience*, **7**, 65.

46 Olah, M., Biber, K., Vinet, J. and Boddeke, H.W. (2011) Microglia phenotype diversity. *CNS Neurol Disord Drug Targets*, **10**, 108-118.

47 Vallieres, N., Berard, J.L., David, S. and Lacroix, S. (2006) Systemic injections of lipopolysaccharide accelerates myelin phagocytosis during Wallerian degeneration in the injured mouse spinal cord. *Glia*, **53**, 103-113.

48 Chen, S., Zhang, H., Pu, H., Wang, G., Li, W., Leak, R.K., Chen, J., Liou, A.K. and Hu, X. (2014) n-3 PUFA supplementation benefits microglial responses to myelin pathology. *Sci. Rep.*, **4**, 7458.

49 Mosley, K. and Cuzner, M.L. (1996) Receptor-mediated phagocytosis of myelin by macrophages and microglia: effect of opsonization and receptor blocking agents. *Neurochem. Res.*, **21**, 481-487.

50 van der Goes, A., Brouwer, J., Hoekstra, K., Roos, D., van den Berg, T.K. and Dijkstra, C.D. (1998) Reactive oxygen species are required for the phagocytosis of myelin by macrophages. *J. Neuroimmunol.*, **92**, 67-75.

51 van der Laan, L.J., Ruuls, S.R., Weber, K.S., Lodder, I.J., Dopp, E.A. and Dijkstra, C.D. (1996) Macrophage phagocytosis of myelin in vitro determined by flow cytometry: phagocytosis is mediated by CR3 and induces production of tumor necrosis factor-alpha and nitric oxide. *J. Neuroimmunol.*, **70**, 145-152.

52 Williams, K., Ulvestad, E., Waage, A., Antel, J.P. and McLaurin, J. (1994) Activation of adult human derived microglia by myelin phagocytosis in vitro. *J. Neurosci. Res.*, **38**, 433-443.

53 Wang, X., Cao, K., Sun, X., Chen, Y., Duan, Z., Sun, L., Guo, L., Bai, P., Sun, D., Fan, J. *et al.* (2015) Macrophages in spinal cord injury: phenotypic and functional change from exposure to myelin debris. *Glia*, **63**, 635-651.

54 Neumann, H., Kotter, M.R. and Franklin, R.J. (2009) Debris clearance by microglia: an essential link between degeneration and regeneration. *Brain : a journal of neurology*, **132**, 288-295.

55 Olah, M., Amor, S., Brouwer, N., Vinet, J., Eggen, B., Biber, K. and Boddeke, H.W. (2012) Identification of a microglia phenotype supportive of remyelination. *Glia*, **60**, 306-321.

56 Dyall, S.C. and Michael-Titus, A.T. (2008) Neurological benefits of omega-3 fatty acids. *Neuromolecular medicine*, **10**, 219-235.

57 Michael-Titus, A.T. and Priestley, J.V. (2014) Omega-3 fatty acids and traumatic neurological injury: from neuroprotection to neuroplasticity? *Trends Neurosci.*, **37**, 30-38.

58 Carta, A.R. and Pisanu, A. (2013) Modulating microglia activity with PPAR-gamma agonists: a promising therapy for Parkinson's disease? *Neurotox. Res.*, **23**, 112-123.

59 Yamanaka, M., Ishikawa, T., Griep, A., Axt, D., Kummer, M.P. and Heneka, M.T. (2012) PPARgamma/RXRalpha-induced and CD36-mediated microglial amyloid-beta phagocytosis results in cognitive improvement in amyloid precursor protein/presenilin 1 mice. *The Journal of neuroscience : the official journal of the Society for Neuroscience*, **32**, 17321-17331.

60 Gushchina, S., Pryce, G., Yip, P.K., Wu, D., Pallier, P., Giovannoni, G., Baker, D. and Bo, X. (2018) Increased expression of colony-stimulating factor-1 in mouse spinal cord with experimental autoimmune encephalomyelitis correlates with microglial activation and neuronal loss. *Glia*, **66**, 2108-2125.

61 Basso, D.M., Beattie, M.S. and Bresnahan, J.C. (1995) A sensitive and reliable locomotor rating scale for open field testing in rats. *Journal of neurotrauma*, **12**, 1-21.

62 Basso, D.M., Fisher, L.C., Anderson, A.J., Jakeman, L.B., McTigue, D.M. and Popovich, P.G. (2006) Basso Mouse Scale for locomotion detects differences in recovery after spinal cord injury in five common mouse strains. *Journal of neurotrauma*, **23**, 635-659.

63 Clark, A.K., Yip, P.K. and Malcangio, M. (2009) The liberation of fractalkine in the dorsal horn requires microglial cathepsin S. *The Journal of neuroscience : the official journal of the Society for Neuroscience*, **29**, 6945-6954.

64 Yip, P.K., Wong, L.F., Sears, T.A., Yanez-Munoz, R.J. and McMahon, S.B. (2010) Cortical overexpression of neuronal calcium sensor-1 induces functional plasticity in spinal cord following unilateral pyramidal tract injury in rat. *PLoS Biol.*, **8**, e1000399.

65 Yip, P.K., Kaan, T.K., Fenesan, D. and Malcangio, M. (2009) Rapid isolation and culture of primary microglia from adult mouse spinal cord. *J. Neurosci. Methods*, **183**, 223-237.

66 Burguillos, M.A., Deierborg, T., Kavanagh, E., Persson, A., Hajji, N., Garcia-Quintanilla, A., Cano, J., Brundin, P., Englund, E., Venero, J.L. *et al.* (2011) Caspase signalling controls microglia activation and neurotoxicity. *Nature*, **472**, 319-324.

67 Norton, W.T. and Poduslo, S.E. (1973) Myelination in rat brain: method of myelin isolation. *Journal of neurochemistry*, **21**, 749-757.

68 Ahmed, Z., Dent, R.G., Suggate, E.L., Barrett, L.B., Seabright, R.J., Berry, M. and Logan, A. (2005) Disinhibition of neurotrophin-induced dorsal root ganglion cell neurite outgrowth on CNS myelin by siRNA-mediated knockdown of NgR, p75NTR and Rho-A. *Mol. Cell Neurosci.*, **28**, 509-523.

69 Greenhalgh, A.D. and David, S. (2014) Differences in the phagocytic response of microglia and peripheral macrophages after spinal cord injury and its effects on cell death. *The Journal of neuroscience : the official journal of the Society for Neuroscience*, **34**, 6316-6322.

70 DeJong, B.A. and Smith, M.E. (1997) A role for complement in phagocytosis of myelin. *Neurochem. Res.*, **22**, 491-498.

71 Ponnusamy, V., Kapellou, O., Yip, E., Evanson, J., Wong, L.F., Michael-Titus, A., Yip, P.K. and Shah, D.K. (2016) A study of microRNAs from dried blood spots in newborns after perinatal asphyxia: a simple and feasible biosampling method. *Pediatric research*, **79**, 799-805.

Figure 1. DHA improves open field locomotor scores in rodent spinal cord contusion injury. (A) DHA-treated Sprague-Dawley rats showed significantly improved locomotor recovery when compared to vehicle-treated animals on days 5, 6, 7, 14, 21 and 28 post-contusion SCI when using the BBB locomotor rating scale. (B) DHA-treated C57BL/6 mice also showed significantly improved locomotor recovery when compared to vehicle-treated animals on days 11 to 35 post-contusion SCI when using the BMS locomotor rating scale. The i.v. dose of DHA was 500 nmol/kg. Results are displayed as the mean ± SEM. * and ** represent $p<0.05$ and $p<0.01$ vs. vehicle-treated animals, respectively.

Figure 2. DHA prevents NeuN immunopositive cell loss in rat and mice after contusion injury. (A-D) The sections rostral and caudal to the injury site of the contused rat spinal cord were immunostained for NeuN and analysed. Insets are enlarged images of the corresponding dashed boxes. (E-G) DHA-treated rats showed significantly increased NeuN immunolabelled cells when compared to vehicle-treated animals at 2 - 6 mm rostral to the injury site at different ventral and intermediate horizontal planes, at 7 days post-injury (dpi). (H-J) DHA-treated rats showed significantly increased NeuN immunolabelled cells when compared to vehicle-treated animals at 2 - 4 mm caudal to the injury site, at 28 dpi. (K-P) The sections rostral and caudal to the injury site of the contused mouse spinal cord were immunostained for NeuN and analysed. Insets are enlarged images of the corresponding dashed boxes. (Q) No difference in the number of NeuN immunolabelled cells was observed between DHA-treated mice and vehicle-treated mice in the ventral horn at 35 dpi. (R) DHA-treated mice showed significantly more NeuN immunolabelled cells in both caudal and rostral regions when compared to vehicle-treated animals at 35 dpi. (S) DHA-treated mice has significantly more neurons 3 mm rostral to the

injury site when both ventral horn and intermediate cord data were combined. Results are displayed as the mean ± SEM. * represent $p<0.05$ vs. vehicle-treated animals. Scale bars = 100 μm. Ventral and intermediate indicate the ventral and intermediate horizontal planes. Insets are enlarged images of the corresponding dashed boxes.

Figure 3. DHA induces regional and temporal differences in microglia/macrophage cell populations after spinal cord contusion injury in rats and mice. (A-B) The microglia/macrophages present rostral and caudal to the injury site of the contused rat spinal cord were immunostained for ED1 and analysed. (C) DHA-treated animals showed significantly increased ED1 immunolabelled cells when compared to vehicle-treated animals at 4 mm in the rostral and caudal directions during the early phase (7 dpi) ($p<0.05$). (D-E) The microglia/macrophage present rostral and caudal to the injury site of the contused rat spinal cord were immunostained for Iba1 and analysed. Insets are enlarged images of the corresponding dashed boxes. (F) DHA-treated animals showed significantly increased Iba-1 immunolabelled cells when compared to vehicle-treated animals at the lesion epicentre and both 2-4 mm in the rostral and caudal directions during the early phase (7 dpi). (G) No significant difference in Iba-1 immunolabelling was observed between DHA- and vehicle-treated animals during the late phase (28 dpi). (H-K) The microglia/macrophages present in gray and white matter rostral and caudal to the injury site of the contused mouse spinal cord were immunostained for Iba1 and analysed. Insets are enlarged images of the corresponding dashed boxes. Arrows indicate Iba1 immunolablled cells. (L) DHA-treated animals showed significantly less gray matter Iba-1 immunolabelling when compared to vehicle-treated animals at the injury epicentre at 35 dpi. (F) DHA-treated animals showed significantly greater white matter Iba-1 immunolabelling when compared to vehicle-

treated animals, but not in any specific rostro-caudal region at 35 dpi. (G) No significant difference was observed when both gray and white matter data were combined. Results are displayed as the mean ± SEM. * represent $p<0.05$ vs. vehicle-treated animals. Scale bars = 100 μm.

Figure 4. DHA enhances M1 and M2 microglia/macrophage expression after spinal cord contusion injury in rats and mice. (A) Schematic diagram showing the rostral and caudal regions examined in the Western blot. (B) The expression levels of CD16/32 and (C) arginase-1 were upregulated after DHA compared to vehicle treatment at 3 dpi in rats. (D) βIII tubulin was used as the protein loading control. (E-F) Data expressed as mean ± SEM from 4 animals per group showed significant differences in CD16/32 and arginase-1 at the injury epicentre. (G-J) The M1 microglia/macrophages immunostained for CD16/32 (arrows) showed that DHA-treated animals had a significant increase in CD16/32 immunolabelled cells when compared to vehicle-treated animals at the injury epicentre in the gray matter and 1 mm caudal in the white matter at 35 days post contusion. (K-N) The M2 microglia/macrophages immunostained for arginase-1 (arrows) demonstrated that DHA-treated animals has a significant increase in arginase-1 immunolabelled cells when compared to vehicle-treated animals at the injury epicentre in the gray and white matter and 1 mm caudal in the gray matter at 35 days post contusion. Results are displayed as the mean ± SEM. * and ** represent $p<0.05$ and $p<0.01$ vs. vehicle-treated animals, respectively. Scale bars = 100 μm. Insets are enlarged images of the corresponding dashed boxes. Nuclei labelled with DAPI are represented in blue.

Figure 5. DHA reduces selectively the number of murine M1 bone marrow-derived macrophages, but does not alter their phagocytic activity. (A-F) The bone marrow-derived macrophages (BMDM) can either be in a non-polarized phenotype (A-B) or be selectively polarized into an M1 phenotype using LPS and IFN-γ (C-D) or M2 phenotype using IL-4 (E-F). (G, I) For the non-polarized (M0) and M2 phenotypes, DHA (1-3 μM) did not significantly alter the number of cells when compared to the control treatment. (H) However, for the M1 phenotype, DHA (3 μM) significantly reduced the number of cells when compared to the control treatment. (J-O) BMDM immunostained for CD16/32 (green) can phagocytose DiI-labelled myelin after 24h co-incubation. There was no significant change in DiI-labelled myelin levels within BMDM treated with 3 μM DHA compared to vehicle treatment at M0 (P), M1 (Q) and M2 (R) phenotypes. Two wells per treatment and four independent experiments were carried out. Results are displayed as the mean ± SEM. * represents $p<0.05$. Scale bars = 100 μm.

Figure 6. DHA reduces microglial phagocytosis of myelin in the white matter in rat spinal cord 7d after contusion. (A-L) Microglia/macrophage immunostained with Iba1 (red) and DAPI (blue) can phagocytose myelin (green) at 7d after spinal cord contusion. (A-F) Vehicle-or DHA-treated animals showed high levels of phagocytosis at the epicentre level. (G-M) Vehicle-treated animals showed a significantly higher level of phagocytosis of myelin compared to DHA-treated animals at 7d after spinal contusion. Arrows illustrate high phagocytosis of myelin and arrowheads illustrate low phagocytosis of myelin. Results are displayed as the mean ± SEM. * and *** represent $p<0.05$ and $p<0.001$ vs vehicle-treated animals, respectively. Scale bars = 50 μm.

Figure 7. DHA increases miR-124 expression in microglia in white matter in rat spinal cord 7d after contusion. (A-F) Microglia/macrophage immunostained with Iba1 (red) and DAPI (blue) have a lower miR-124 expression (green) in the vehicle-treated group compared to DHA-treated animals. (G) A significant increase in miR-124 expression was observed at the injury epicentre and rostral regions along the spinal cord. Arrows indicate microglia with miR-124 expression. Results are displayed as the mean ± SEM. *, ** and *** represent $p<0.05$, $p<0.01$ and $p<0.001$, vs. vehicle-treated animals, respectively. Scale bars = 100 μm.

Figure 8. DHA reduces microglial phagocytosis of myelin via miR-124 predominantly in the white matter of mouse spinal cord 7d after contusion. (A) Mice receiving DHA and intraspinal negative control injections (blue line) showed a significantly improved locomotor activity when compared to animals receiving vehicle and the negative control (red line), DHA with the miR-124 inhibitor (blue-dashed line), and vehicle with the miR-124 inhibitor (red-dashed line) when using the BMS locomotor rating scale, (B-K) DHA treated mice with intraspinal negative control injections showed significantly fewer co-localisations of MBP positive myelin (red, white arrows) within microglia immunostained with P2Y12 (green) compared to the other treatment groups, in particular, in the rostral (F) and caudal (H), but not the epicentre (G) white matter regions at or near contusion site. No significant change was observed in the rostral (I) and caudal (K), and majority of the epicentre (J) grey matter regions at or near contusion site. Results are displayed as the mean ± SEM. † represent $p<0.05$, **, ^^ and †† represent $p<0.01$, and ††† and ^^^ represent $p<0.001$. *, †, ^ symbols represent Vehicle with negative control, Vehicle with miR-124 inhibitor,

and DHA with miR-124 inhibitor compared against DHA + negative control, respectively. Scale bars = 100 μm.

Figure 9. DHA increases microglial miR-124 predominantly in the white matter of mouse spinal cord 7d after contusion. (A-C) Contused mice with vehicle and intraspinal negative control injections showed limited miR-124 (red, arrow heads) expression within microglia immunostained with P2Y12 (green, arrows) and Hoechst (blue). (D-F) However, animals receiving DHA treatment and intraspinal negative control injections exhibited a significant increase in miR-124 expression within the microglial cells. (G-L) In mice treated with the intraspinal miR-124 inhibitor, limited miR-124 was detected in both the vehicle- and DHA-treated mice. In particular, the rostral (M), epicentre (N) and caudal (O) white matter regions at or near the contusion site showed DHA induced miR-124, which was reduced with the miR-124 inhibitor. (P-R) In the grey matter regions at or near the contusion site, some specific cord regions also showed significant differences between the groups. Results are displayed as the mean ± SEM. *, **, *** represent $p<0.05$, $p<0.01$, and $p<0.001$ respectively. Scale bars = 100 μm.

Figure 10. DHA reduces microglial phagocytosis of myelin debris via miR-124 in primary adult microglial and microglial BV2 cell cultures. (A-F) Primary microglia from adult rat spinal cord immunostained with Iba1 (green) can phagocytose myelin labelled with DiI (red) after 24 h co-incubation. (G) DHA-treated primary microglia exhibited a significant decrease in DiI-labelled myelin when compared to vehicle-treated microglia at 1 μM DHA. (H-I) This significant reduction in phagocytosis correlated with the upregulation of miR-124, but not miR-155. Four independent

experiments were carried out. (J-L) BV2 microglial cells immunostained with IB4 (green) and Hoechst (blue) can phagocytose myelin labelled with DiI (red) after 24 h co-incubation. (M) DHA-treated BV2 microglial cells exhibited a significant decrease in DiI-labelled myelin when compared to vehicle-treated microglia at 3 μM DHA. (L-M) In the presence of the miR-124 inhibitor, the reduced microglial phagocytosis was abolished. Results are displayed as the mean ± SEM. * and *** represent $p<0.05$ and $p<0.001$. Scale bars = 100 μm.

Figure 11. DHA reduces microglial BV2 cell phagoptosis of UV-stressed neuronal PC12 cells. (A) In the absence of DHA, UV-stressed neuronal PC12 cells at the start of the experiment (0 min post co-incubation) express live mitochondria (stained red with TMRE) and nuclei (stained blue with Hoechst). Within 18 min of cell-cell contact with a microglial BV2 cell (stained green with CMFDA), the expression of TMRE is diminished and thereafter 'engulfed' by the microglial BV2 cell by 180 min post co-incubation. (B) In the presence of DHA (3 μM), even after prolonged cell-cell contact between a UV-stressed neuronal PC12 cell and a microglial BV2 cell, the neuronal PC12 cells remained alive and not engulfed. (C) A significant reduction in the percentage of UV-stressed neuronal PC12 cells was observed with microglial BV2 cells in the presence of DHA (1-3 μM). Results are displayed as the mean ± SEM. * represent $p<0.05$. Scale bars = 50 μm.

Suppl. Figure 1. Increased M1 and M2 expression on the ipsilateral compared to the contralateral side of a mouse spinal cord after 7 d post lateral hemisection. (A-C) CD16/32 immunostaining (green), which represents the M1 phenotype was absent at rostral (A) and caudal

(C) levels, and limited in the ipsilateral side (indicated by *) compared to the contralateral side at the epicentre (B, G) region. (D-F) Arginase 1 immunostaining (green) which represents the M2 phenotype was absent at rostral (A) and caudal (C), but a lot higher on the ipsilateral (indicated by *) compared to contralateral side at the epicentre (E, H) region. Results are displayed as the mean ± SEM. Scale bars = 500 μm.

Suppl. Figure 2. Annexin V expression is increased in neuronal PC12 cell cultures after ultraviolet exposure. (A) Neuronal PC12 cells in the absence of UV exposure show limited annexin V (green) expression. (B-C) After exposure of neuronal PC12 cells to UV exposure (200 kJ), there was a significant increase in annexin V expression. Three independent experiments were carried out. Results are displayed as the mean ± SEM. *** represent $p<0.001$. Scale bars = 50 μm.

Figure 1

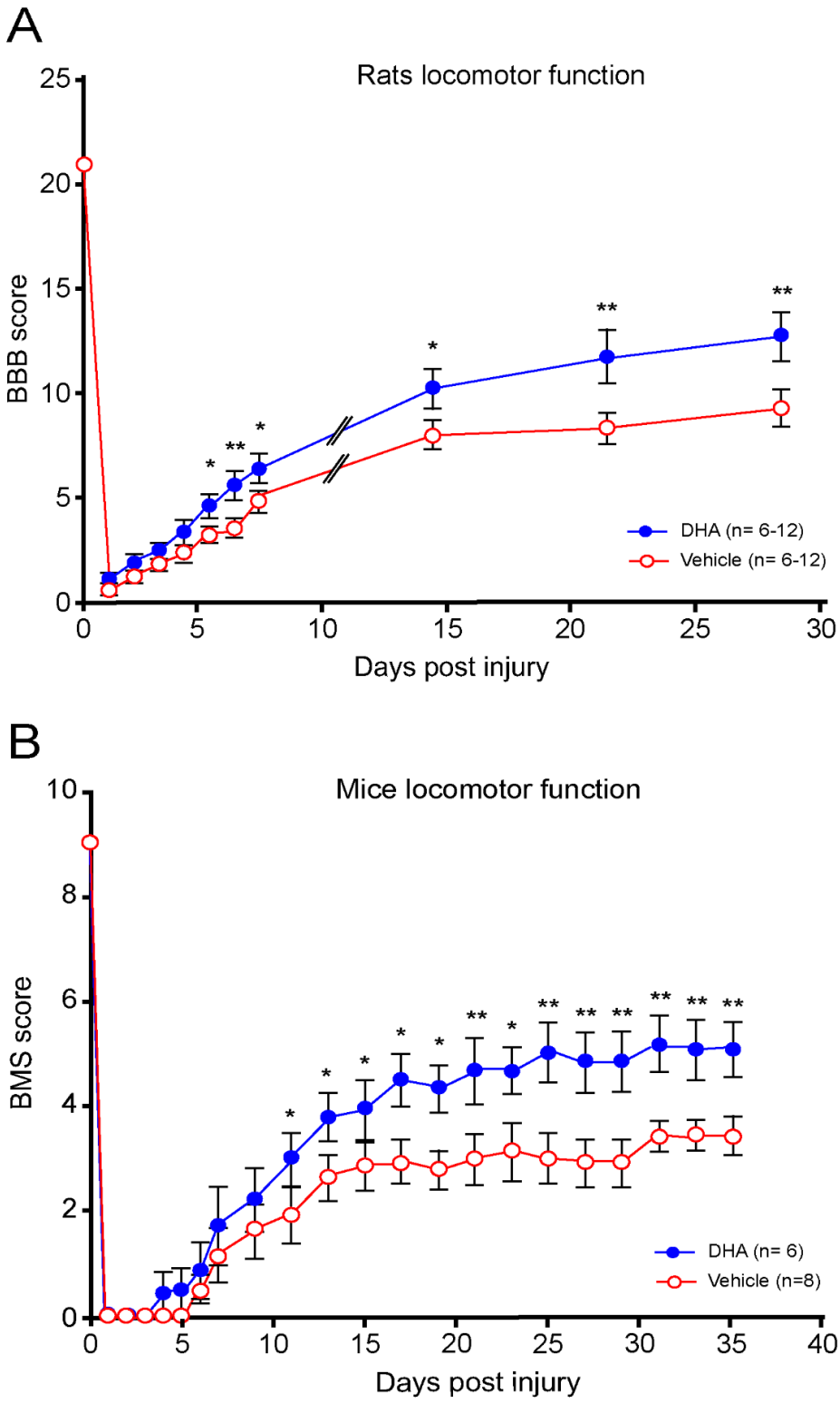
A
Rats locomotor function
BBB score
Days post injury
DHA (n= 6-12)
Vehicle (n= 6-12)
B
Mice locomotor function
BMS score
Days post injury
DHA (n= 6)
Vehicle (n=8)

Figure 2

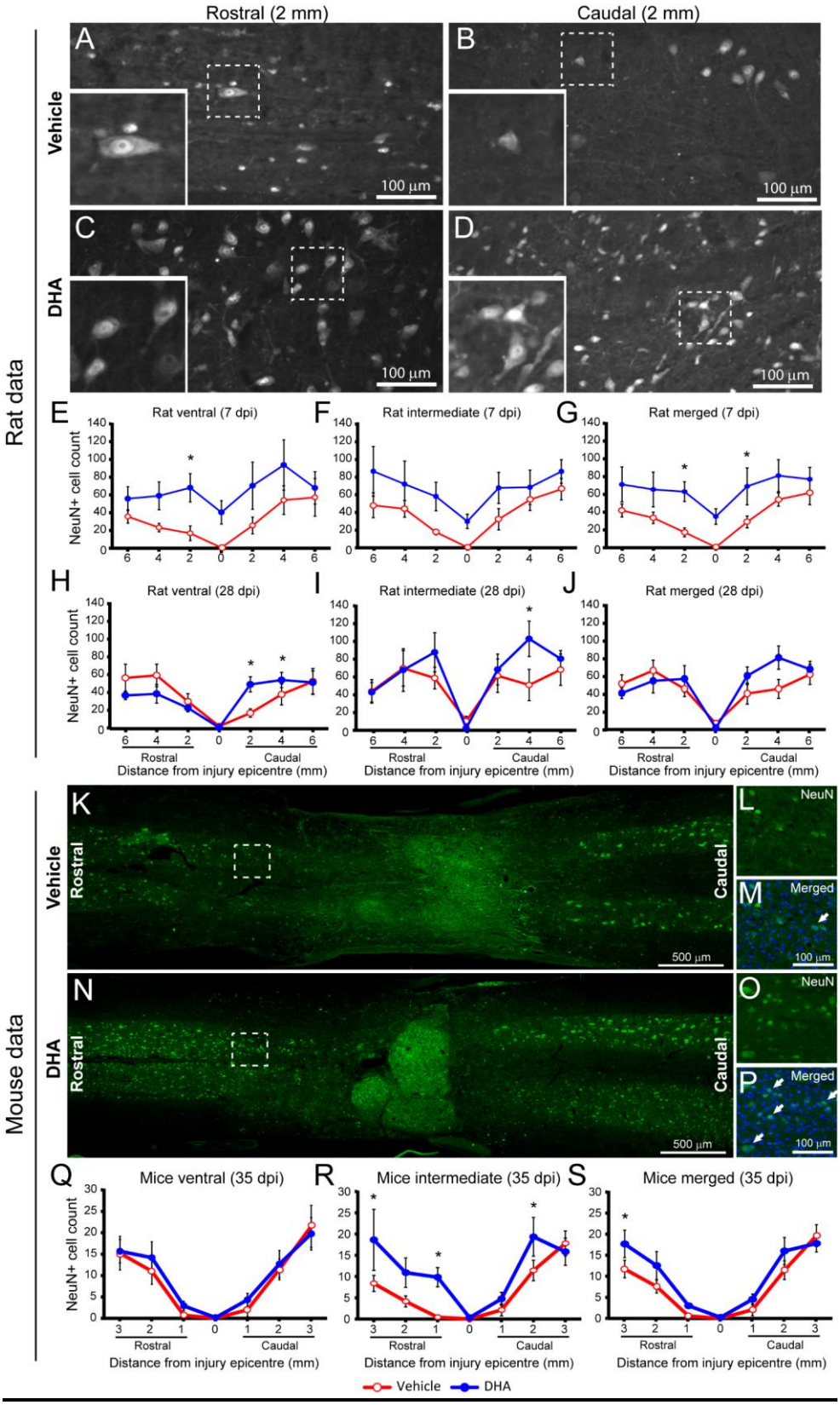
Rostral (2 mm)
Caudal (2 mm)
Rat data
Vehicle
DHA
A
B
C
D
100 µm
E
F
G
H
I
J
Rat ventral (7 dpi)
Rat intermediate (7 dpi)
Rat merged (7 dpi)
Rat ventral (28 dpi)
Rat intermediate (28 dpi)
Rat merged (28 dpi)
NeuN+ cell count
Rostral
Caudal
Distance from injury epicentre (mm)
Mouse data
K
L
M
N
O
P
NeuN
Merged
500 µm
Q
R
S
Mice ventral (35 dpi)
Mice intermediate (35 dpi)
Mice merged (35 dpi)
Vehicle
DHA

Figure 3

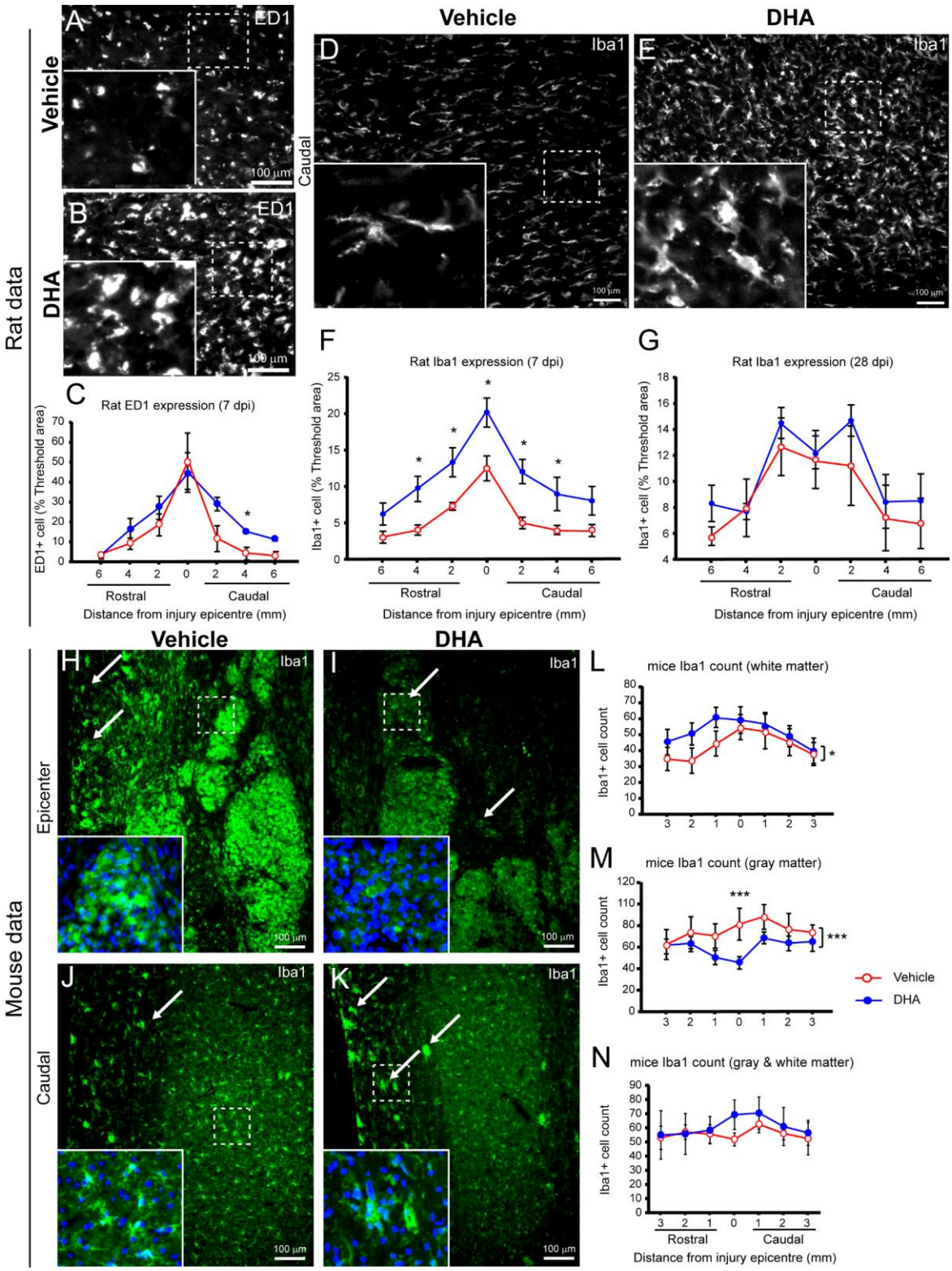
Rat data
Mouse data
Vehicle
DHA
Caudal
Epicenter
A
B
C
D
E
F
G
H
I
J
K
L
M
N
ED1
Iba1
100 µm
Rat ED1 expression (7 dpi)
ED1+ cell (% Threshold area)
Rat Iba1 expression (7 dpi)
Iba1+ cell (% Threshold area)
Rat Iba1 expression (28 dpi)
Rostral
Caudal
Distance from injury epicentre (mm)
mice Iba1 count (white matter)
mice Iba1 count (gray matter)
mice Iba1 count (gray & white matter)
Iba1+ cell count
Vehicle
DHA

Figure 4

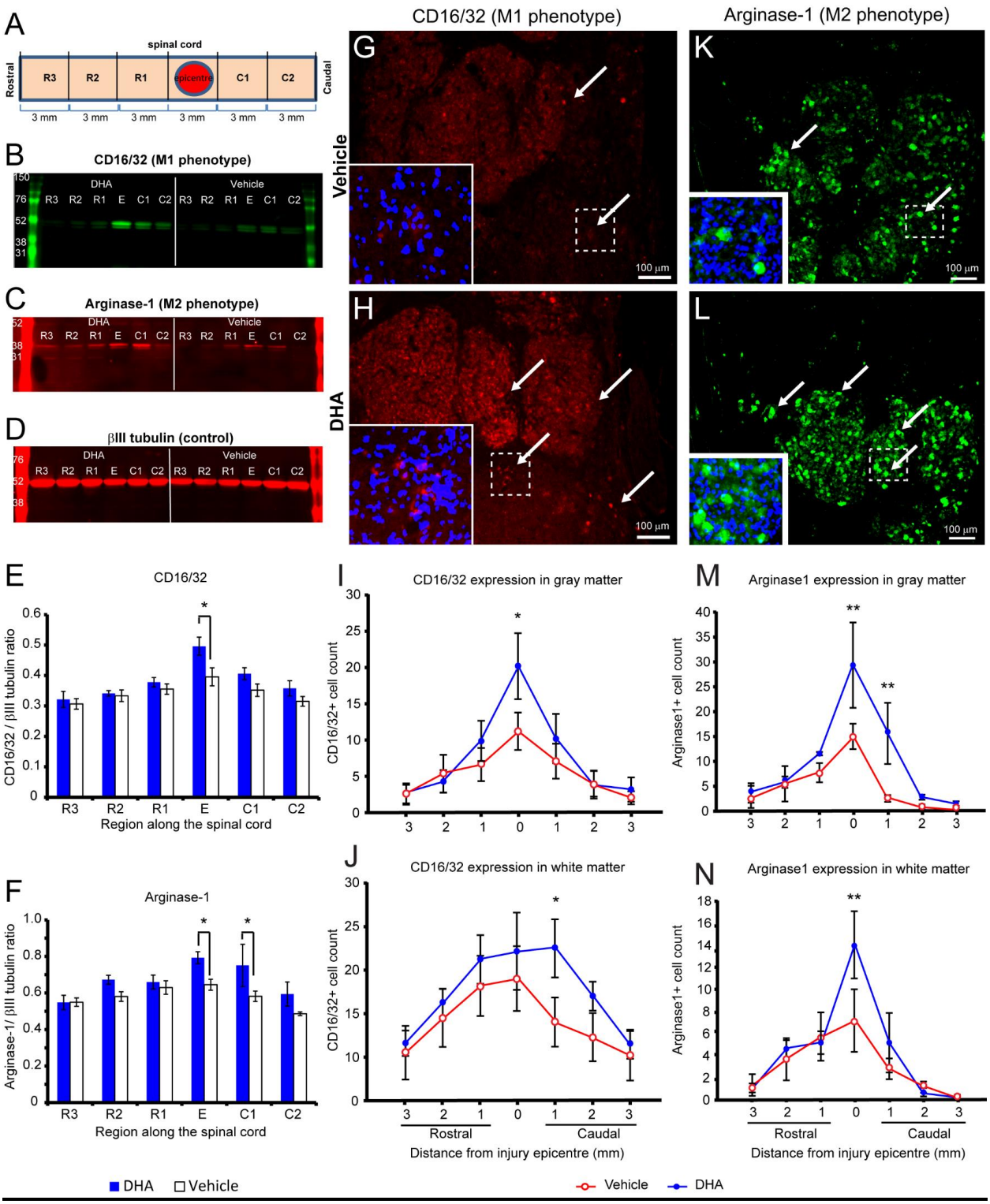
A
spinal cord
Rostral
R3
R2
R1
epicentre
C1
C2
Caudal
3 mm
B
CD16/32 (M1 phenotype)
DHA
Vehicle
C
Arginase-1 (M2 phenotype)
D
βIII tubulin (control)
CD16/32 (M1 phenotype)
Arginase-1 (M2 phenotype)
Vehicle
DHA
100 μm
E
CD16/32
CD16/32 / βIII tubulin ratio
Region along the spinal cord
F
Arginase-1
Arginase-1/ βIII tubulin ratio
I
CD16/32 expression in gray matter
CD16/32+ cell count
J
CD16/32 expression in white matter
Rostral
Caudal
Distance from injury epicentre (mm)
M
Arginase1 expression in gray matter
Arginase1+ cell count
N
Arginase1 expression in white matter
DHA
Vehicle

Figure 5

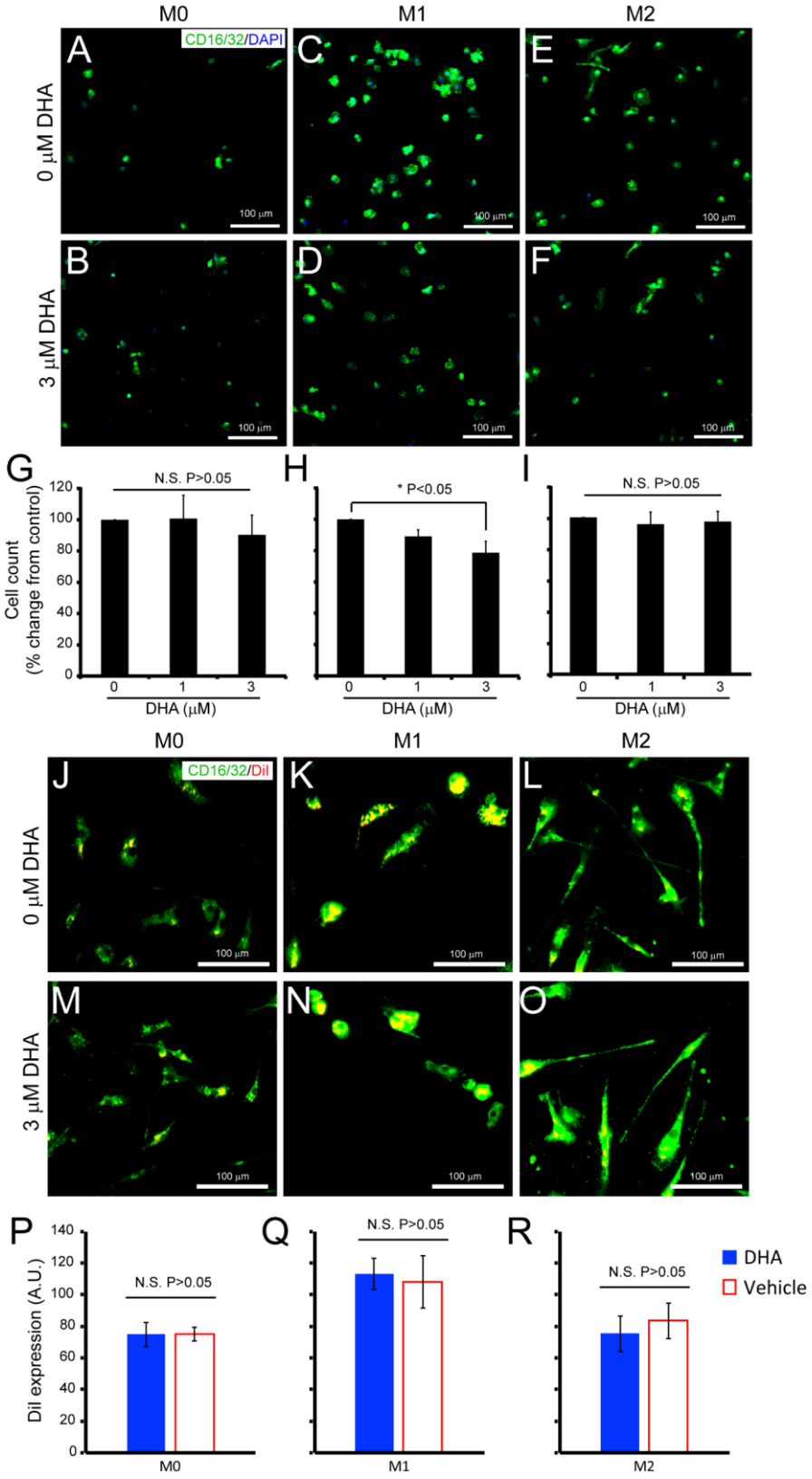
M0
M1
M2
CD16/32/DAPI
A
C
E
0 μM DHA
B
D
F
3 μM DHA
100 μm
G
H
I
N.S. P>0.05
* P<0.05
N.S. P>0.05
Cell count
(% change from control)
120
100
80
60
40
20
0
0
1
3
DHA (μM)
M0
M1
M2
CD16/32/DiI
J
K
L
0 μM DHA
M
N
O
3 μM DHA
100 μm
P
Q
R
N.S. P>0.05
N.S. P>0.05
N.S. P>0.05
DHA
Vehicle
DiI expression (A.U.)
140
120
100
80
60
40
20
0
M0
M1
M2

Figure 6

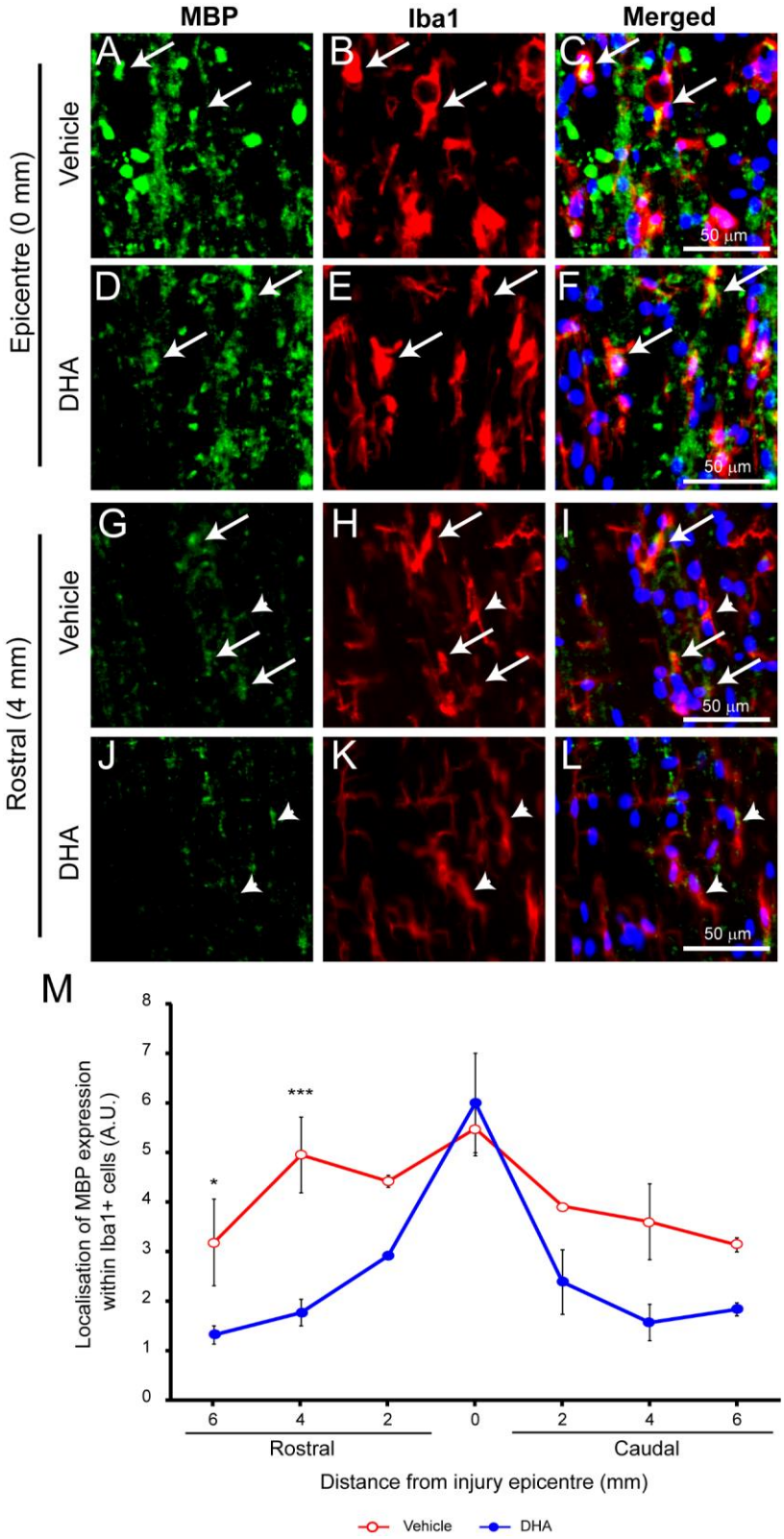
MBP
Iba1
Merged
A
B
C
D
E
F
G
H
I
J
K
L
Epicentre (0 mm)
Rostral (4 mm)
Vehicle
DHA
50 µm
M
Localisation of MBP expression within Iba1+ cells (A.U.)
*
***
Rostral
Caudal
Distance from injury epicentre (mm)
Vehicle
DHA

Figure 7

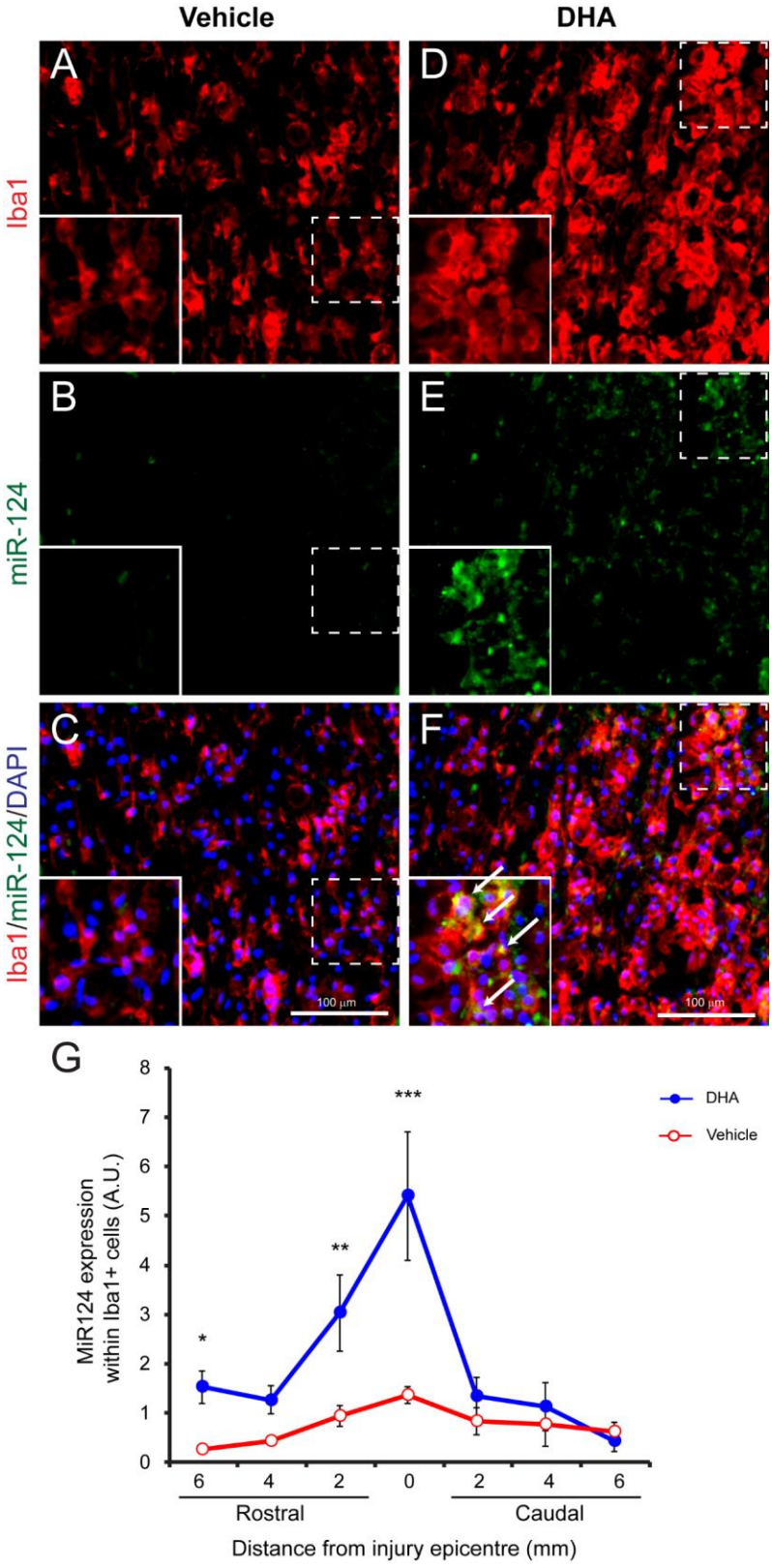
Vehicle
DHA
A
D
Iba1
B
E
miR-124
C
F
Iba1/miR-124/DAPI
100 µm
100 µm
G
MiR124 expression within Iba1+ cells (A.U.)
DHA
Vehicle
*
**
***
Rostral
Caudal
Distance from injury epicentre (mm)

Figure 8

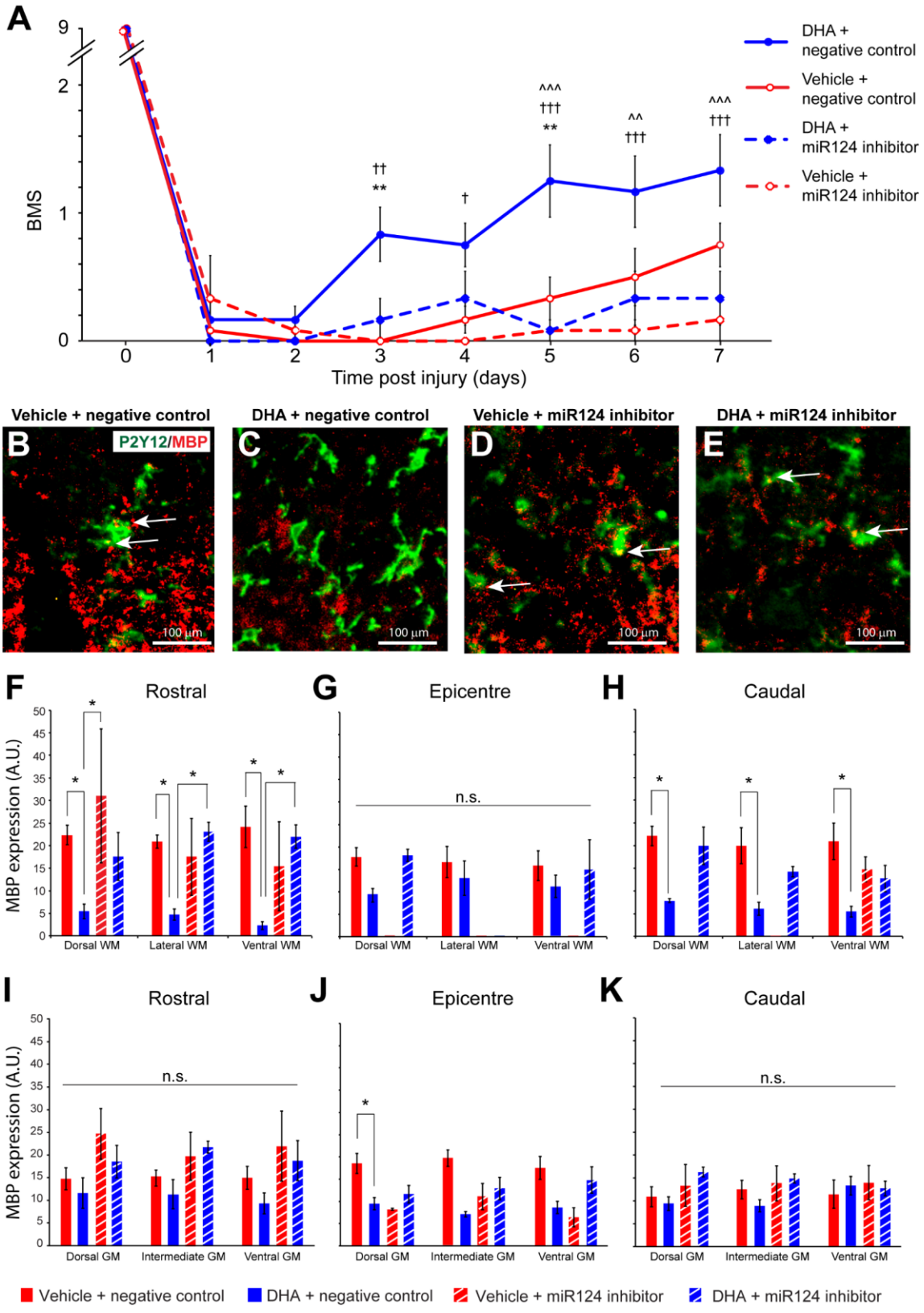
A
BMS
Time post injury (days)
DHA + negative control
Vehicle + negative control
DHA + miR124 inhibitor
Vehicle + miR124 inhibitor
Vehicle + negative control
DHA + negative control
Vehicle + miR124 inhibitor
DHA + miR124 inhibitor
B
C
D
E
P2Y12/MBP
100 µm
F
Rostral
G
Epicentre
H
Caudal
MBP expression (A.U.)
Dorsal WM
Lateral WM
Ventral WM
n.s.
I
Rostral
J
Epicentre
K
Caudal
Dorsal GM
Intermediate GM
Ventral GM
Vehicle + negative control
DHA + negative control
Vehicle + miR124 inhibitor
DHA + miR124 inhibitor

Figure 9

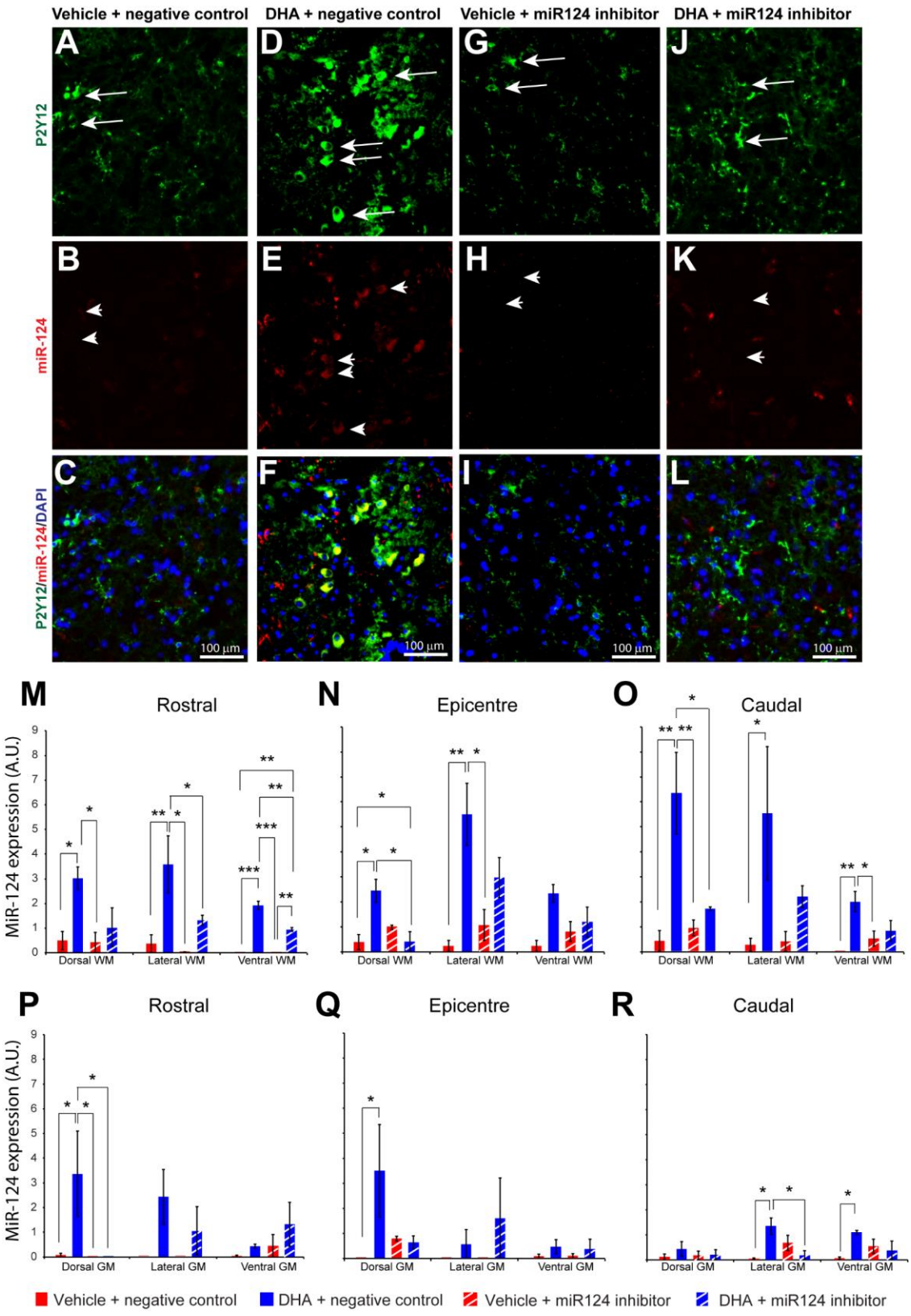
Vehicle + negative control
DHA + negative control
Vehicle + miR124 inhibitor
DHA + miR124 inhibitor
A
D
G
J
P2Y12
B
E
H
K
miR-124
C
F
I
L
P2Y12/miR-124/DAPI
100 µm
M
Rostral
N
Epicentre
O
Caudal
MiR-124 expression (A.U.)
Dorsal WM
Lateral WM
Ventral WM
P
Rostral
Q
Epicentre
R
Caudal
MiR-124 expression (A.U.)
Dorsal GM
Lateral GM
Ventral GM
Vehicle + negative control
DHA + negative control
Vehicle + miR124 inhibitor
DHA + miR124 inhibitor

Figure 10

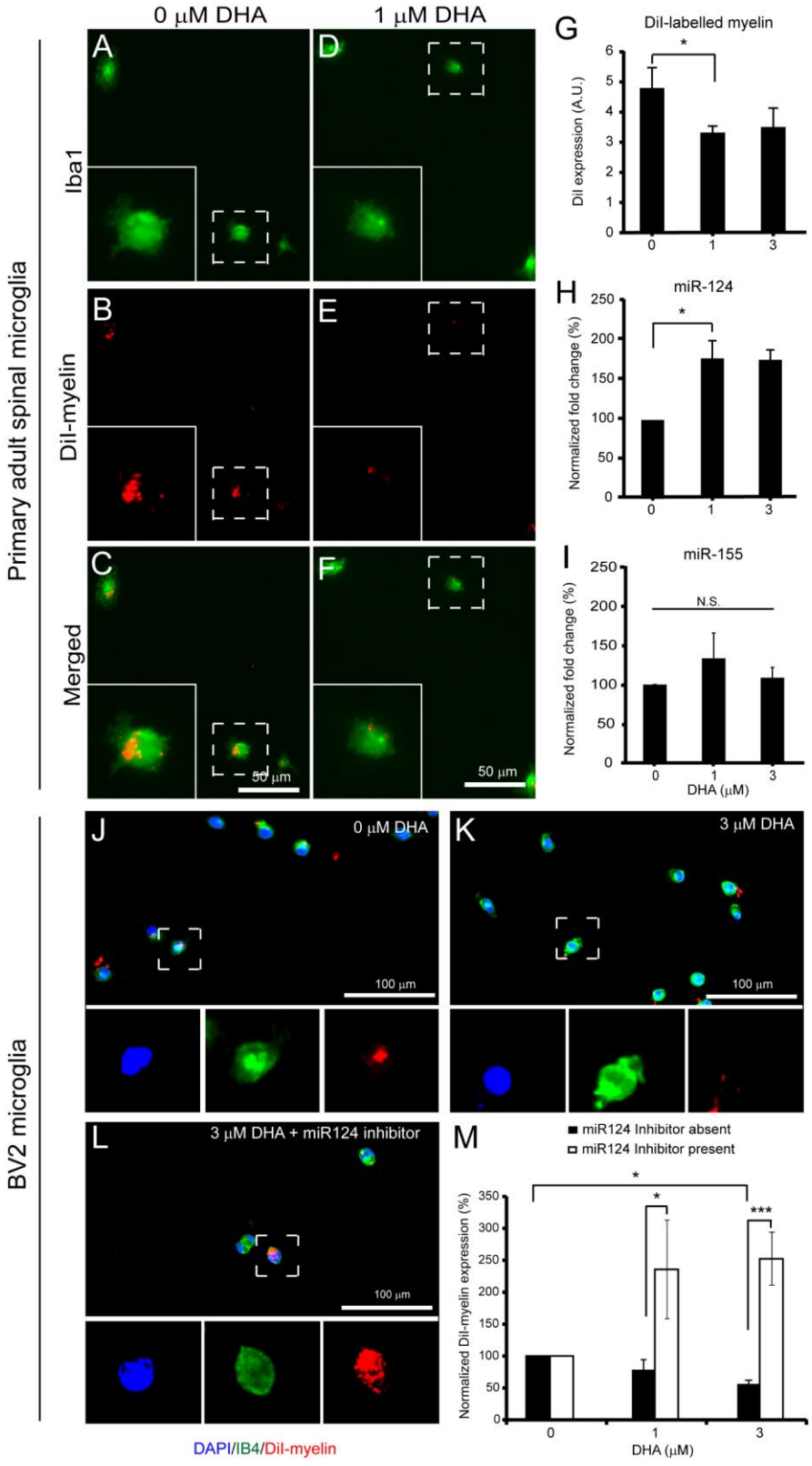
0 μM DHA
1 μM DHA
Primary adult spinal microglia
Iba1
Dil-myelin
Merged
A
B
C
D
E
F
50 μm
G
Dil-labelled myelin
Dil expression (A.U.)
H
miR-124
Normalized fold change (%)
I
miR-155
N.S.
DHA (μM)
BV2 microglia
J
0 μM DHA
K
3 μM DHA
100 μm
L
3 μM DHA + miR124 inhibitor
M
miR124 Inhibitor absent
miR124 Inhibitor present
Normalized Dil-myelin expression (%)
DAPI/IB4/Dil-myelin

Figure 11

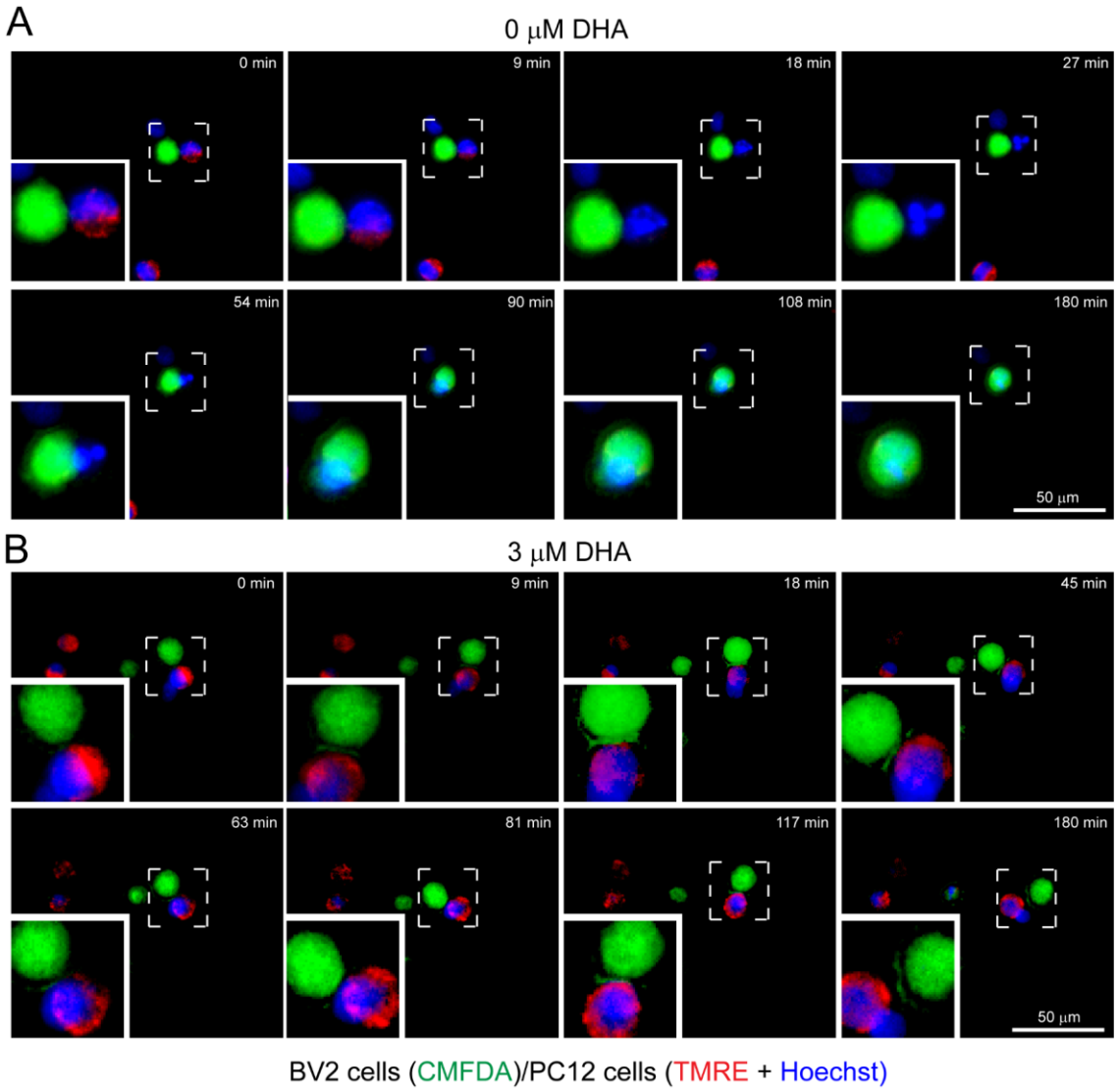
A
0 μM DHA
0 min
9 min
18 min
27 min
54 min
90 min
108 min
180 min
50 μm
B
3 μM DHA
0 min
9 min
18 min
45 min
63 min
81 min
117 min
180 min
50 μm
BV2 cells (CMFDA)/PC12 cells (TMRE + Hoechst)
C
*
*
Phagoptosis of UV-stressed PC12 cells (% of contact)
70
60
50
40
30
20
10
0
0
1
3
DHA (μM)

Suppl. Fig. 1

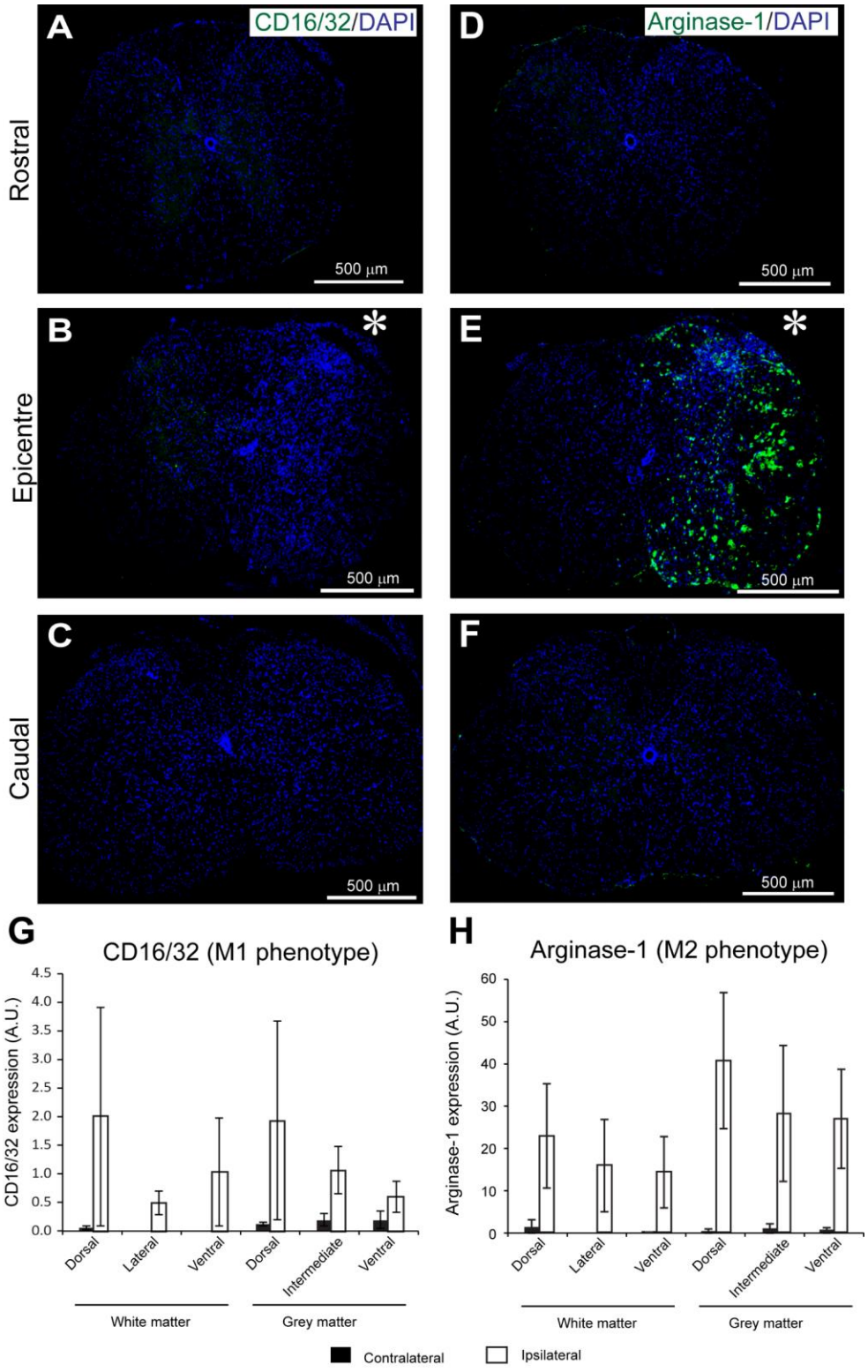
A
CD16/32/DAPI
D
Arginase-1/DAPI
Rostral
500 μm
B
E
Epicentre
C
F
Caudal
G
CD16/32 (M1 phenotype)
CD16/32 expression (A.U.)
H
Arginase-1 (M2 phenotype)
Arginase-1 expression (A.U.)
Dorsal
Lateral
Ventral
Intermediate
White matter
Grey matter
Contralateral
Ipsilateral

Suppl. Fig. 2

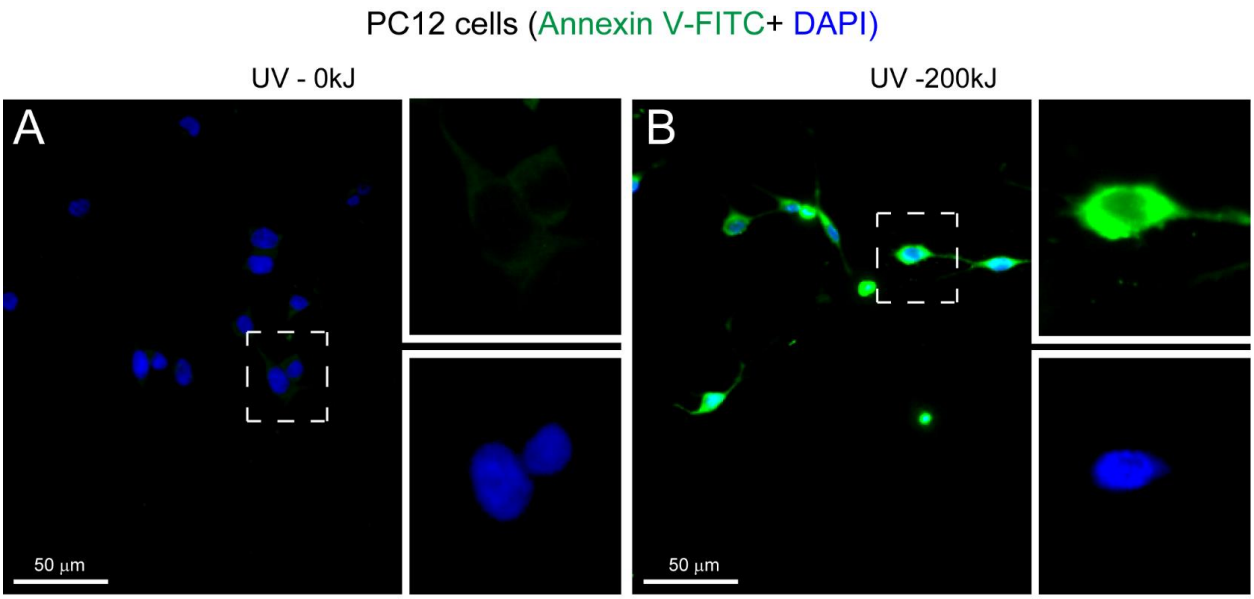
PC12 cells (Annexin V-FITC+ DAPI)
UV - 0kJ
UV -200kJ
A
B
50 µm
50 µm

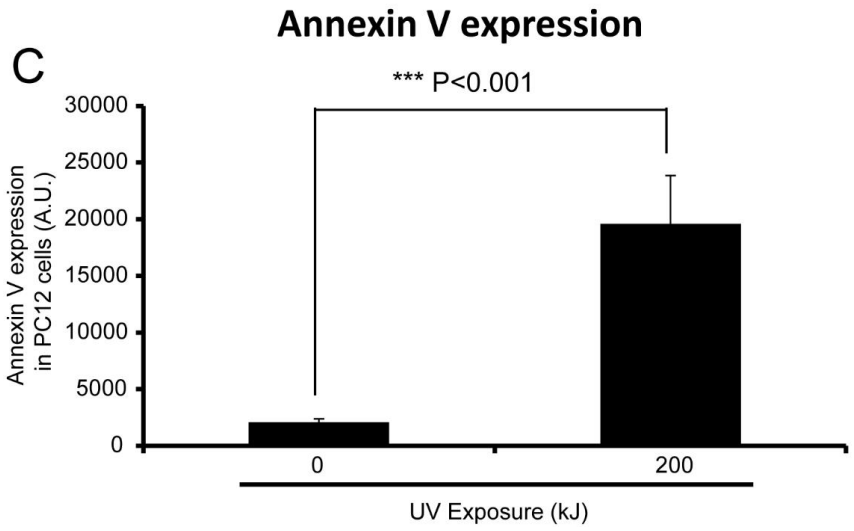
C
Annexin V expression
*** P<0.001
Annexin V expression in PC12 cells (A.U.)
30000
25000
20000
15000
10000
5000
0
0
200
UV Exposure (kJ)